

# Journal of Visualized Experiments

## Surface Mapping of Earth-like Exoplanets using Single Point Light Curves

--Manuscript Draft--

<b>Article Type:</b>	Invited Methods Article - JoVE Produced Video
<b>Manuscript Number:</b>	JoVE60951R3
<b>Full Title:</b>	Surface Mapping of Earth-like Exoplanets using Single Point Light Curves
<b>Section/Category:</b>	JoVE Engineering
<b>Keywords:</b>	Planetary Science; Astronomical spectroscopy; Exoplanets; Exoplanet surface variability; Planetary surface characteristics; Earth-like exoplanets
<b>Corresponding Author:</b>	Siteng Fan California Institute of Technology Pasadena, CA UNITED STATES
<b>Corresponding Author's Institution:</b>	California Institute of Technology
<b>Corresponding Author E-Mail:</b>	stfan@gps.caltech.edu
<b>Order of Authors:</b>	Siteng Fan Yuk L. Yung
<b>Additional Information:</b>	
<b>Question</b>	<b>Response</b>
Please indicate whether this article will be Standard Access or Open Access.	Standard Access (US\$2,400)
Please indicate the <b>city, state/province, and country</b> where this article will be <b>filmed</b> . Please do not use abbreviations.	Pasadena, California, United States

**TITLE:**

Surface Mapping of Earth-like Exoplanets using Single Point Light Curves

**AUTHORS AND AFFILIATIONS:**

Siteng Fan, Yuk L. Yung

Division of Geological and Planetary Sciences, California Institute of Technology, Pasadena, CA, USA

Email addresses of co-authors:

Yuk L. Yung ([yly@gps.caltech.edu](mailto:yly@gps.caltech.edu))

Corresponding author:

Siteng Fan ([stfan@gps.caltech.edu](mailto:stfan@gps.caltech.edu))

**KEYWORDS:**

Planetary Science; Astronomical spectroscopy; Exoplanets; Exoplanet surface variability; Planetary surface characteristics; Earth-like exoplanets

**SUMMARY:**

The protocol extracts information from light curves of exoplanets and constructs their surface maps. It uses light curves of Earth, which serves as a proxy exoplanet, to demonstrate the approach.

**ABSTRACT:**

Spatially resolving exoplanet features from single-point observations is essential for evaluating the potential habitability of exoplanets. The ultimate goal of this protocol is to determine whether these planetary worlds harbor geological features and/or climate systems. We present a method of extracting information from multi-wavelength single-point light curves and retrieving surface maps. It uses singular value decomposition (SVD) to separate sources that contribute to light curve variations and infer the existence of partially cloudy climate systems. Through analysis of the time series obtained from SVD, physical attributions of principal components (PCs) could be inferred without assumptions of any spectral properties. Combining with viewing geometry, it is feasible to reconstruct surface maps if one of the PCs are found to contain surface information. Degeneracy originated from convolution of the pixel geometry and spectrum information determines the quality of reconstructed surface maps, which requires the introduction of regularization. For the purpose of demonstrating the protocol, multi-wavelength light curves of Earth, which serves as a proxy exoplanet, are analyzed. Comparison between the results and the ground truth is presented to show the performance and limitation of the protocol. This work provides a benchmark for future generalization of exoplanet applications.

**INTRODUCTION:**

Identifying habitable worlds is one of the ultimate goals in astrobiology<sup>1</sup>. Since the first detection<sup>2</sup>, more than 4000 exoplanets have been confirmed to date<sup>3</sup> with a number of Earth

analogs (e.g., TRAPPIST-1e)<sup>4</sup>. These planets have orbital and planetary properties similar to those of Earth, and therefore are potentially habitable. Evaluating their habitability from limited observations is essential in this context. Based on the knowledge of life on Earth, geological and climate systems are critical to habitability, which can therefore serve as biosignatures. In principle, features of these systems could be observed from a distance even when a planet could not be spatially resolved better than one single point. In this case, identifying geological features and climate systems from single-point light curves is essential when assessing the habitability of exoplanets. Surface mapping of these exoplanets becomes urgent.

Despite the convolution between viewing geometry and spectral features, information of an exoplanet's surface is contained in its time-resolved single-point light curves, which can be obtained from a distance, and derived with sufficient observations. However, two-dimensional (2D) surface mapping of potentially habitable Earth-like exoplanets is challenging due to the influence of clouds. Methods of retrieving 2D maps have been developed and tested using simulated light curves and known spectra<sup>5-8</sup>, but they have not been applied to real observations. Moreover, in the analyses of exoplanet observations now and in the near future, assumptions of characteristic spectra may be controversial when the planetary surface compositions are not well-constrained.

In this paper, we demonstrate a surface mapping technique for Earth-like exoplanets. We use SVD to evaluate and separate information from different sources that is contained in multi-wavelength light curves without assumptions of any specific spectra. Combined with viewing geometry, we present the reconstruction of surface maps using timely resolved but spatially convoluted surface information. For the purpose of demonstrating this method, two-year multi-wavelength single-point observations of Earth obtained by the Deep Space Climate Observatory/Earth Polychromatic Imaging Camera (DSCOVR/EPIC; [www.nesdis.noaa.gov/DSCOVR/spacecraft.html](http://www.nesdis.noaa.gov/DSCOVR/spacecraft.html)) are analyzed. We use Earth as a proxy exoplanet to assess this method because currently available observations of exoplanets are not sufficient. We attach the code with the paper as an example. It is developed under python 3.7 with anaconda and healpy packages, but the mathematics of the protocol can also be done in other programming environments (e.g., IDL or MATLAB).

## PROTOCOL:

### 1. Programming setup

1.1. Set up the programming environment for the attached code. A computer with Linux operating system is required, as the healpy package is not available on Windows. The code is not computationally expensive, so a normal personal computer can handle the protocol.

1.2. Follow the instruction (<https://docs.anaconda.com/anaconda/install/linux/>) to install Anaconda with Python 3.7 onto the system, then use the following commands in terminal to set up the programming environment:

```
$ conda create --name myenv python=3.7
```

```
89 $ conda activate myenv
90 $ conda install anaconda
91 $ conda install healpy
92
```

NOTE: These steps may take minutes depending on the hardware and Internet speed. The environment name 'myenv' in the first two command lines can be changed to any other string.

## 2. Obtaining multi-wavelength light curves and viewing geometry from observations

2.1. In the viewing geometry, include the longitude and latitude of the sub-stellar and the sub-observer points for each corresponding time frame.

To use the following attached code, ensure that these two files have the same format as **LightCurve.csv** and **Geometry.csv**.

2.2. Run **PlotTimeSeries.py** to visualize the data and check their qualities. Two figures **LightCurve.png** and **Geometry.png** will be created (**Supplemental Figure 1-2**). Parameters in this and following plotting codes may need to be adjusted if applied to different observations.

```
$ python PlotTimeSeries.py LightCurve
$ python PlotTimeSeries.py Geometry
```

## 3. Extract surface information from light curves

3.1. Center time-resolved multi-wavelength albedo light curves of an exoplanet and normalize them by corresponding standard deviation at each wavelength. This results in the equal importance of each channel.

$$R'_{t,k} = \frac{R_{t,k} - \mu_k}{\sigma_k}$$

where  $R'_{t,k}$  and  $R_{t,k}$  are the scaled and observed albedo at the  $t$ -th time step and the  $k$ -th wavelength, respectively;  $\mu_k$  and  $\sigma_k$  are the mean and standard deviation of the albedo time series at the  $k$ -th wavelength.

3.1.1. Run **Normalize.py** to normalize the light curves,  $R_{t,k}$ . The output is saved in **NormalizedLightCurve.csv**.

```
$ python Normalize.py
```

3.2. Run **PlotTimeSeries.py** to visualize the normalized light curves. A figure **NormalizedLightCurve.png** will be created (**Supplemental Figure 3**).

```
$ python PlotTimeSeries.py NormalizedLightCurve
```

3.3. Apply SVD on the scaled albedo light curves to find dominant PCs and their corresponding time series.

$$\mathbf{R}'_{[T \times K]} = \mathbf{U}_{[T \times K]} \mathbf{\Sigma}_{[K \times K]} \mathbf{V}_{[K \times K]}^T$$

On the left hand side,  $T$  and  $K$  are the total number of time steps and observation wavelengths;



$\mathbf{R}'$  is the matrix of scaled albedo observations, whose (t,k)-th element is  $R'_{t,k}$ . On the right hand side, columns of  $\mathbf{V}$  are PCs, orthonormal vectors that define the space SVD projects to;  $\mathbf{\Sigma}$  is a diagonal matrix, whose (k,k)-th element is the standard deviation of scaled light curves along the k-th axis defined by the k-th column of  $\mathbf{V}$ ; columns of  $\mathbf{U}$  are the corresponding time series of each PC in  $\mathbf{V}$ .

3.3.1. Run `SingularValueDecomposition.py` to decompose  $\mathbf{R}'$ . The resulting  $\mathbf{U}$ ,  $\mathbf{\Sigma}$ ,  $\mathbf{V}^T$  are saved in the output files **U.csv**, **SingularValue.csv** and **V\_T.csv**, respectively.

```
$ python SingularValueDecomposition.py
```

3.4. Use **PlotTimeSeries.py** and **PlotSVD.py** to visualize the SVD result. Three figures **U.png**, **Sigma.png** and **V\_T.png** will be created (**Supplemental Figure 4-6**).

```
$ python PlotTimeSeries.py U
```

```
$ python PlotSVD.py
```

3.5. Analyze contributions and corresponding time series of PCs to determine the one that contains surface information.

3.5.1. Compare the singular values at the diagonal of  $\mathbf{\Sigma}$ . An Earth-like partially cloudy exoplanet is expected to have two comparable dominant singular values.

NOTE:  $\mathbf{\Sigma}$  may contain less or more than two dominant singular values, which is discussed below.

3.5.2. Compare the time series patterns of the two dominant PCs. The PC that contains surface information tends to have more regular shape than the other. Due to the longitudinal asymmetry and the reappearance of surface with small changes in two consecutive days, the corresponding time series tends to have approximately constant daily variation.

3.5.3. Compute the periodicities of the two dominant PCs using Lomb-Scargle periodogram<sup>9,10</sup> to confirm the selection of PC. The PC that contains surface information tends to have higher peak corresponding to rotation period in the power density spectrum.

3.5.4. Run **Periodogram.py** to obtain the power spectra of the time series of each PC. The power spectra are saved in **Periodogram.csv**.

```
$ python Periodogram.py
```

3.5.5. Run **PlotPeriodogram.py** to visualize these periodograms and confirm the selection of PC. A figure **Periodogram.png** will be created (**Supplemental Figure 7**). The current plotting code adds in dashed lines representing annual, semi-annual, diurnal and half-daily cycles for reference, which may need to be changed when applied to other observations.

```
$ python PlotPeriodogram.py
```

3.5.6. Select the PC,  $\mathbf{v}_j$ , that contains surface information and its time series,  $\mathbf{u}_j$ .

$$\mathbf{v}_{j[K \times 1]} = \mathbf{V}_{[K \times K]}[:, j]$$

where  $\mathbf{V}[:,j]$  and  $\mathbf{U}[:,j]$  are the  $j$ -th columns of  $\mathbf{V}$  and  $\mathbf{U}$ , respectively;  $j$  is the index of PC inferred at step 3.3 that contains surface information.

#### 4. Construct planetary surface map

4.1. Use the Hierarchical Equal Area iso-Latitude Pixelization (HEALPix)<sup>11</sup> method to pixelate the retrieving map. It divides spherical surface of a planet into pixels with the same area and uniform distribution. Denote the unknown value of the  $p$ -th pixel as  $x_p$ .

4.1.1. Run **HEALPixRandom.py** to visualize the pixelization method. A figure **HEALPixRandom.png** will be created (**Supplemental Figure 8**). The parameter  $N_{\text{side}}$  at line 17 can be changed for different resolutions. This step may take a few seconds to minutes depending on the resolution.

```
$ python HEALPixRandom.py
```

4.2. Compute the weight of the  $p$ -th pixel in observations at the  $t$ -th time step,  $w_{t,p}$ , using viewing geometry.

$$w_{t,p} = \begin{cases} c_t \cos(\alpha_{t,p}) \cos(\beta_{t,p}) & \text{when } \alpha_{t,p} < 90^\circ \text{ and } \beta_{t,p} < 90^\circ \\ 0 & \text{otherwise} \end{cases}$$

where  $\alpha_{t,p}$ ,  $\beta_{t,p}$  are the solar and the spacecraft zenith angles at the pixel;  $c_t$  is a normalization term of the  $t$ -th observation so that sum of the total weight at each time step is unity.

NOTE: Geometry is assumed to be known at this step, or can be derived from other analysis, which is discussed below.

4.2.1. Run **ComputeWeight.py** to compute  $w_{t,p}$ . Change the value of  $N_{\text{side}}$  at line 23 for other resolutions of the retrieved map. The output is saved as **W.npz** due to its size.

```
$ python ComputeWeight.py
```

4.3. Use **PlotWeight.py** to visualize these weights. A number of figures, one at each time step, will be created in a folder **Weight**. Merging them results in **Supplemental Video 1**, which shows how the weight of each pixel changes with time. The first command line takes minutes depending on the resolution, and the second may take hours to finish due to the large number of visualizations.

```
$ python PlotWeight.py
```

4.4. Combine geometry and observations to reach a linear regression problem.

$$\mathbf{W}_{[T \times P]} \mathbf{x}_{[P \times 1]} = \mathbf{u}_{j[T \times 1]}$$

where  $P$  is the total number of retrieving pixels;  $\mathbf{W}$  is the weight matrix with  $w_{t,p}$  as the  $(t,p)$ -th element;  $\mathbf{x}$  consists of  $x_p$  as the  $p$ -th element, which is the quantity to be solved in this problem.

Solve the linear regression problem with a regularization of L-2 norm.

$$\mathbf{x} = (\mathbf{W}^T \mathbf{W} + \lambda \mathbf{I})^{-1} \mathbf{W}^T \mathbf{u}_j$$

where  $I$  is the identity matrix and  $\lambda$  is the regularization parameter.

NOTE:  $10^{-3}$  is a good value for  $\lambda$  when  $T \sim 10^4$  and  $P \sim 3 \times 10^3$ . They should be adjusted by comparing the values of the two terms in the regularized square error,  $e$ , as shown below.

$$e = \|Wx - u_j\|_2^2 + \lambda \|x\|_2^2$$

4.4.1. Run **LinearRegression.py** to solve this linear regression problem. The result of  $x$  is saved in the file **PixelValue.csv**. Change the value of  $\lambda$  at line 16 for different strengths of regularization.  
\$ python LinearRegression.py

4.5. Convert  $x$  to a 2D surface map according to the mapping rule of HEALPix.

4.5.1. Run **PlotMap.py** to construct the retrieved maps using different regularization parameters. Three figures **Map\_-2.png**, **Map\_-3.png** and **Map\_-4.png** will be created with the current setting (**Supplemental Figure 9**). The relationship between the pixel indices and their locations on map is described in the HEALPix document<sup>11</sup>. This step takes tens of seconds.  
\$ python PlotMap.py

## 5. Estimate uncertainty of the retrieved map

5.1. Rewrite the linear regression problem at step 4.3 with the “true value” of  $x$  as  $z$  and the observation noise,  $\epsilon$ .

$$W_{[T \times P]} z_{[P \times 1]} + \epsilon_{[T \times 1]} = u_{j[T \times 1]}$$

5.1.1. Assume  $\epsilon$  to follow a Gaussian Distribution  $\mathcal{N}(0, \sigma^2 I_{[T \times T]})$  and estimate its covariance.  $T-P$  is the degree of freedom of  $u_j$  from observation when the retrieved map is fixed.

$$\sigma^2 = \frac{(u_j - Wx)^T (u_j - Wx)}{T - P}$$

5.1.2. Combine equations in step 4.4 and 5.1. It results in a Gaussian vector of  $x$ .

$$x = (W^T W + \lambda I)^{-1} (W^T W) z + (W^T W + \lambda I)^{-1} W^T \epsilon$$

5.1.3. Compute the expectation and the covariance matrix of  $x$ .

$$E[x] = (W^T W + \lambda I)^{-1} (W^T W) z$$
$$Cov[x] = \sigma^2 (W^T W + \lambda I)^{-1} W^T W (W^T W + \lambda I)^{-1}$$

5.1.4. Obtain the uncertainty of each element in  $x$  as the square root of the corresponding element on the diagonal of **Cov[x]**.

$$e_p = \sqrt{Diag[Cov[x]]_p}$$

where  $e_p$  is the uncertainty of  $x_p$ ; **Diag[Cov[x]]<sub>p</sub>** is  $p$ -th element on the diagonal of **Cov[x]**.

5.1.5. Run ‘Covariance.py’ to compute the covariance matrix of  $x$ . The result is saved in

'Covariance.npz' due to its size. This step takes tens of seconds to minutes depending on the size of  $\mathbf{W}$ .

```
$ python Covariance.py
```

5.2. Convert  $\mathbf{e}_p$  to the retrieved 2D map according to the mapping rule of HEALPix.

5.2.1. Run **PlotCovariance.py** to visualize  $\mathbf{Cov}[\mathbf{x}]$  and map the uncertainty  $\mathbf{e}_p$  to the retrieved map. Two figures **Covariance.png** and **Uncertainty.png** will be created (**Supplemental Figure 10-11**).

```
$ python PlotCovariance.py
```

## REPRESENTATIVE RESULTS:

We use multi-wavelength single-point light curves of Earth to demonstrate the protocol, and compare the results with the ground truth to evaluate the quality of surface mapping. Observation used here is obtained by DSCOVR/EPIC, which is a satellite located near the first Lagrangian point (L1) between Earth and Sun taking images at ten wavelengths of the sunlit face of Earth. Two years (2016 and 2017) of observations are used for this demonstration, which are the same as those in Jiang et al. (2018)<sup>12</sup> and Fan et al. (2019)<sup>13</sup>, where more details about the observations are presented. A sample observation at 9:27 UTC, 2017 February 8 is shown in **Figure 1**. Images of Earth are integrated to single points to simulate light curve observations obtained by Aliens, distant observers, who could not spatially resolve Earth better than one pixel. Therefore, multi-wavelength single-point exoplanet light curves with  $\sim 10,000$  time steps are generated, which are the input data of this protocol.

Following step 3, we find two dominant PCs in the multi-wavelength light curves, and the second PC (PC2) contains surface information. Derived as step 3.5, time series of PC2 shows more regular morphology with an approximately constant daily variation, and its power spectrum shows stronger diurnal cycle than the first PC (PC1, **Figure 2**). Therefore, a surface map of this proxy exoplanet is constructed following step 4 (**Figure 3a**), which consists of the value of PC2 at each pixel. Compared with the ground truth of Earth (**Figure 3b**), the reconstructed map recovers all major continents, despite some disagreements in the southern hemisphere where clouds partially prevent surface information from being observed. Uncertainty of each pixel value obtained according to step 5 (**Figure 3c**) is on the order of 10% of that in the retrieved map, suggesting a good quality of the surface mapping and a positive result.

## FIGURE AND TABLE LEGENDS:

**Figure 1. Reflectance images of Earth's sunlit hemisphere.** The observations are taken by DSCOVR/EPIC at ten wavelengths and at 9:27 UTC, 2017 February 8.

**Figure 2. Time series and power spectra of the two dominant PCs.** (a) Time series of PC1. Daily maximum and minimum are denoted by black lines. (b) Power spectrum of PC1's time series. Annual, semi-annual, diurnal and half-daily cycles are denoted as black dashed line. (c) and (d) are identical to (a) and (b), but correspond to PC2. This figure is taken from Fan et al. (2019)<sup>13</sup>.

**Figure 3. Reconstruction of Earth's surface.** (a) Surface map of Earth, which serves as a proxy exoplanet, reconstructed from multi-wavelength light curves. Colors in the map are the values of PC2 at each pixel. The contour of median value is denoted as the black line. (b) Ground truth of Earth's surface map. (c) Uncertainty of the reconstructed map shown in (a). This figure is modified from Fan et al. (2019)<sup>13</sup>.

**Figure 4. Result of finding the optimal regularization parameter.** The optimal value of the regularization parameter  $\lambda$  is  $10^{-3.153}$  (dashed line) when  $\chi^2$  of the reconstruction (solid line) reaches its minimum.

**Figure 5. Sensitivity test of observation noise.** (a) Correlation coefficient between PC2 and land fraction in the field of view (solid line) derived from observations with different signal to noise ratios (S/Ns). The original correlation from light curves without noise is shown as the dashed line. (b) The importance of each PC on the land fraction derived with different observation S/Ns. The importance is computed using Gradient Boosted Regression Trees (GBRT) models as described in Fan et al. (2019)<sup>13</sup>.

#### **SUPPLEMENTARY FILES:**

**Supplemental Figure 1. Time series of reflectance of Earth at ten wavelengths.**

**Supplemental Figure 2. (a) Time series of latitude of the sub-observer point. (b) Same as (a), but for longitude. (c) and (d) are identical to (a) and (b), but correspond to the sub-stellar point.**

**Supplemental Figure 3. Time series of normalized reflectance of Earth at ten wavelengths.**

**Supplemental Figure 4. Time series of the ten PCs, columns of U.**

**Supplemental Figure 5. Singular values corresponding to each PC, diagonal elements of  $\Sigma$ .**

**Supplemental Figure 6. Normalized reflectance spectra of ten PCs, columns of V.**

**Supplemental Figure 7. Power density spectra of time series of ten PCs.**

**Supplemental Figure 8. Pixelization of retrieving map, filled with random pixel values.**

**Supplemental Figure 9. Reconstructed map of Earth using different regularization parameters of (a)  $10^{-2}$ , (b)  $10^{-3}$ , and (c)  $10^{-4}$ .**

**Supplemental Figure 10. Covariance matrix of  $x$ .**

**Supplemental Figure 11. Square root of the diagonal elements of the covariance matrix of  $x$ , mapped onto the retrieved surface map.**

**Video S1. Pixel weights for observations at each time frame in 2016 and 2017.**

## DISCUSSION:

One critical requirement of the protocol is the feasibility of extracting surface information from light curves, which depends on the cloud coverage. In step 3.5.1, the relative values of the PCs may be different among exoplanets. In the case of Earth, the first two PCs dominate the light curve variations, and correspond to surface-independent clouds and surface (Fan et al. 2019)<sup>13</sup>. They have comparable singular values so that the surface information can be separated following steps 3.5.2 and 3.5.3. For a future observation of exoplanet, in extreme cases of either an entirely cloudy or a cloud-free exoplanet, only one dominant PC would appear in the SVD at step 3.3. Spectral analysis is necessary in this case to interpret the meaning of this PC, as compositions of clouds and surface are different. If the dominant PC corresponds to the surface, step 4 and 5 could still be followed; if it corresponds to clouds, a conclusion can be drawn that surface information is blocked by clouds and therefore cannot be extracted using light curves at any wavelengths. In this case, surface mapping is not feasible. A third or even fourth comparable dominant PC may also exist, which can correspond to another layer of clouds or large-scale hydrological processes, and would not invalidate the following steps of the method as long as the surface information is extracted.

Degeneracy resulting from the convolution of geometry and spectrum is the dominant factor that constrains the quality of the retrieved map, as discussed in Cowan & Strait (2013)<sup>14</sup> and Fujii et al. (2017)<sup>15</sup>. As the time series of dominant PCs cover only a small portion of the PC plane, there is always a trade-off between spatial and spectral variations. In other words, the retrieved map (**Figure 2a**) could not be much improved even with an infinite number of time steps and perfect observations, as long as using light curves at the same wavelengths. We introduce the regularization to partially relieve the degeneracy. The optimal value of the regularization term  $\lambda$  in step 4.4 is determined using observations synthesized by the ground truth, where the observed  $\mathbf{u}_j$  is replaced by weighted and scaled land fractions in the field of view (FOV). To generate the synthetic observation, we use the equation at step 4.3 and replace  $\mathbf{x}$  with the ground truth land fractions of each pixel,  $\mathbf{y}$ .  $\mathbf{y}$  is scaled to the same range with  $\mathbf{x}$  using the strong linear correlation between PC2 of observation,  $\mathbf{u}_2$ , and the averaged FOV land fraction<sup>13</sup>. Due to the degeneracy,  $\mathbf{y}$  cannot be perfectly recovered from the linear regression in step 4.4, so we determine the optimal value of  $\lambda$  by finding the minimum of  $\chi^2$ , squared residual scaled by the variance of each pixel. The latter is estimated by the absolute value of each pixel. This is similar to the L-curve criterion in Kawahara & Fujii (2011)<sup>16</sup>. In the particular case of this paper where  $T=9739$  and  $P=3072$ , the optimal value of  $\lambda$  is  $10^{-3.153}$  (**Figure 4**).

Observation noise, another factor that influences the mapping quality, may corrupt the SVD analysis of light curves in practical. We test the robustness of the protocol by introducing different levels of observation noise to the original light curves. They are assumed to contain all noise sources (e.g. sky background, dark current and readout noise), and follow Gaussian distribution. In the original light curves without noise, PC2 shows strong ( $r^2=0.91$ ) linear correlation with the FOV land fraction<sup>13</sup>, so its time series is used for the surface mapping. With increasing noise level, the correlation between PC2 and surface becomes weaker (**Figure 5**). The correlation coefficient,  $r^2$ , becomes below 0.5 when the signal to noise ratio (S/N) is less than 10

(Figure 5a), although the importance of PC2 is still dominant (Figure 5b). We suggest a minimum S/N of 30 for confidently applying the protocol in future generalization. It is worth noting that S/N here is the ratio of exoplanet signal to the observation noise, with the signal of parent star being removed.

Viewing geometry is assumed to be known at step 4.2, as precisely deriving viewing geometry from exoplanet observations is beyond the scope of this work. Besides the orbital elements that can be derived from light curve observations, and rotation period from power density spectra (Figure 2b and 2d), there are only two quantities, summer/winter solstice and obliquity, that are required for surface mapping. Summer/winter solstice usually coincide with extremum of time series of the surface corresponding PC, as long as there exists noticeable asymmetry between northern and southern hemispheres. Obliquity of the exoplanet can be inferred from its influence on the amplitude and frequency of light curves<sup>17,18</sup>. All these derivations require observations sampling frequency at least higher than that of planetary rotation, which is currently rarely satisfied for exoplanets.

#### ACKNOWLEDGMENTS:

This work was partly supported by the Jet Propulsion Laboratory, California Institute of Technology, under contract with NASA. YLY acknowledge support by the Virtual Planetary Laboratory at the University of Washington.

#### DISCLOSURES:

The authors have nothing to disclose.

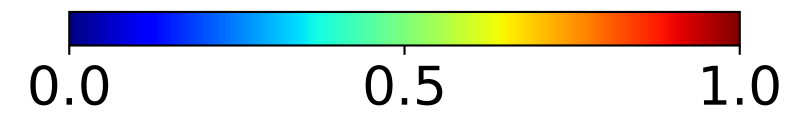
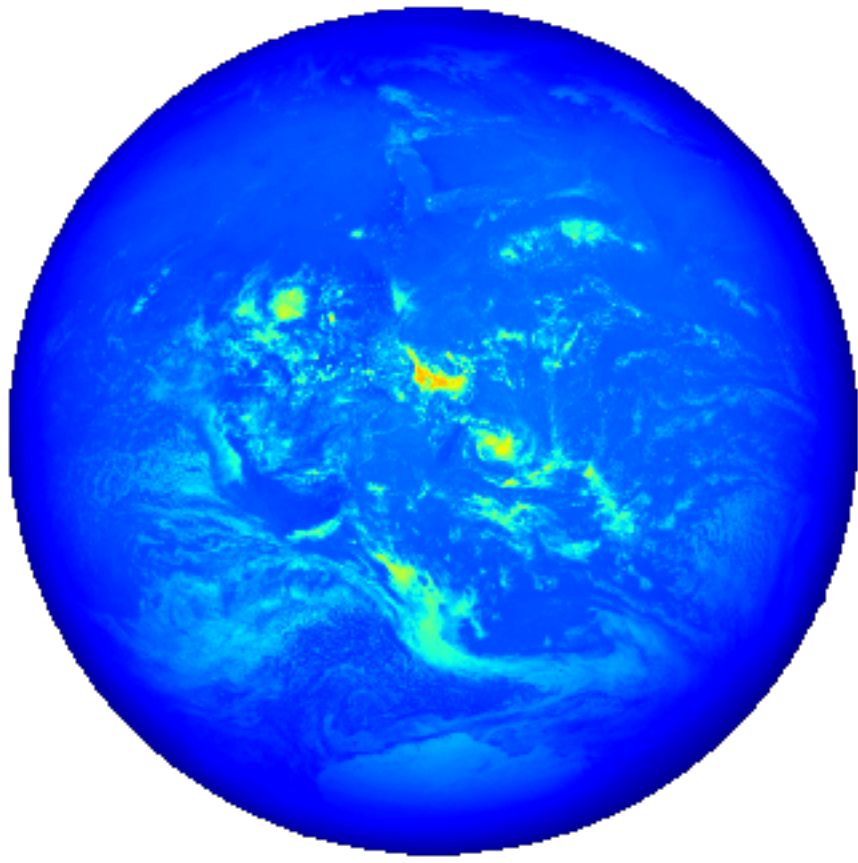
#### REFERENCES:

1. Schwieterman, E. W., et al. Exoplanet Biosignatures: A Review of Remotely Detectable Signs of Life. *Astrobiology*. **18** (6), 663-708 (2018).
2. Campbell, B., Walker, G. A. H., Yang, S. A Search for Substellar Companions to Solar-type Stars. *The Astrophysical Journal*. **331**, 902 (1988).
3. NASA Exoplanet Archive (2019) Confirmed Planets Table, doi:10.26133/NEA1
4. Gillon, M., et al. Seven temperate terrestrial planets around the nearby ultracool dwarf star TRAPPIST-1. *Nature*. **542** (7642), 456-460 (2017).
5. Kawahara, H., Fujii, Y. Global Mapping of Earth-like Exoplanets from Scattered Light Curves. *The Astrophysical Journal*. **720** (2), 1333 (2010).
6. Fujii, Y., Kawahara, H. Mapping Earth Analogs from Photometric Variability: Spin-Orbit Tomography for Planets in Inclined Orbits. *The Astrophysical Journal*. **755** (2), 101 (2012).
7. Cowan, N. B., Fujii, Y. Mapping Exoplanets in *Handbook of Exoplanets*. Springer, Cham. (2018).
8. Farr, B., Farr, W. M., Cowan, N. B., Haggard, H. M., Robinson, T. exocartographer: A Bayesian Framework for Mapping Exoplanets in Reflected Light. *The Astronomical Journal*. **156** (4), 146 (2018).
9. Lomb, N. R. Least-Squares Frequency Analysis of Unequally Spaced Data. *Astrophysics and Space Science*. **39** (2), 447 (1976).
10. Scargle, J. D. Studies in astronomical time series analysis. II. Statistical aspects of spectral analysis of unevenly spaced data. *The Astrophysical Journal*. **263**, 835 (1982).

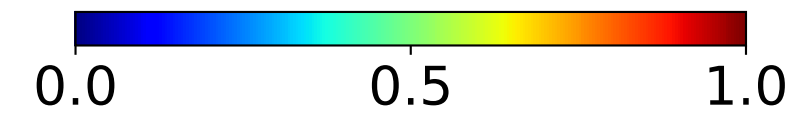
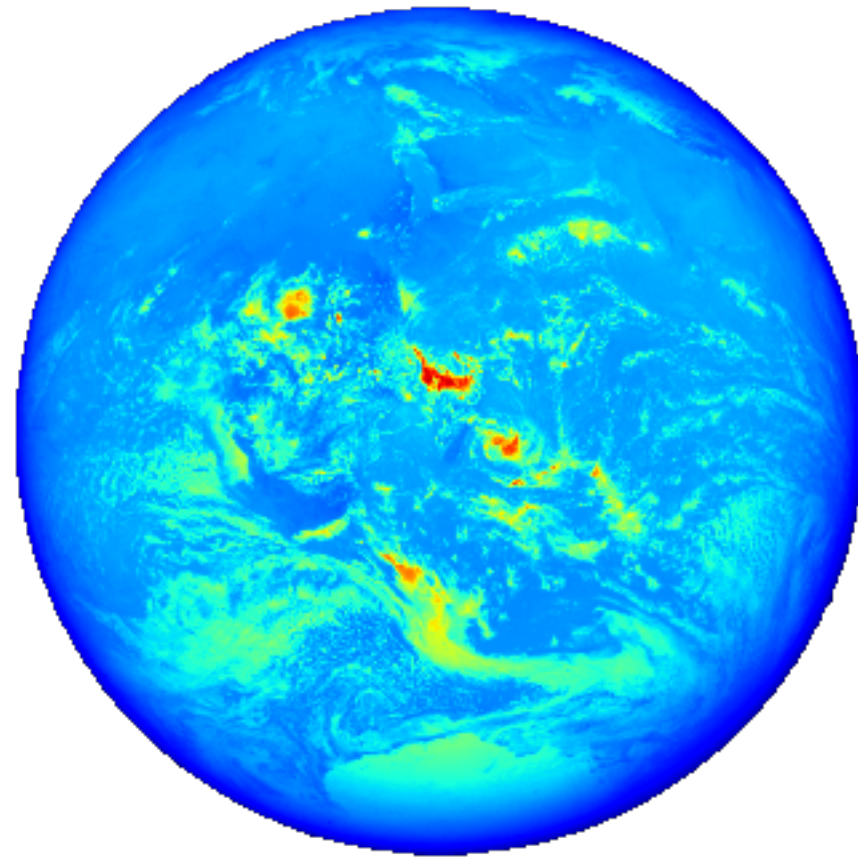
- 436 11. Górski, K. M., et al. HEALPix: A Framework for High-Resolution Discretization and Fast Analysis  
437 of Data Distributed on the Sphere. *The Astrophysical Journal*. **622** (2), 759 (2005).
- 438 12. Jiang, J. H., et al. Using Deep Space Climate Observatory Measurements to Study the Earth as  
439 an Exoplanet. *The Astronomical Journal*. **156** (1), 26 (2018).
- 440 13. Fan, S., et al. Earth as an Exoplanet: A Two-dimensional Alien Map. *The Astrophysical Journal*  
441 *Letters*. **882** (1), L1 (2019).
- 442 14. Cowan, N. B., Strait, T. E. Determining Reflectance Spectra of Surfaces and Clouds on  
443 Exoplanets. *The Astrophysical Journal Letters*. **765** (1), L17 (2013).
- 444 15. Fujii, Y., Lustig-Yaeger, J., Cowan, N. B. Rotational Spectral Unmixing of Exoplanets:  
445 Degeneracies between Surface Colors and Geography. *The Astronomical Journal*. **154** (5), 189  
446 (2017).
- 447 16. Kawahara, H., Fujii, Y. Mapping Clouds and Terrain of Earth-like Planets from Photometric  
448 Variability: Demonstration with Planets in Face-on Orbits. *The Astrophysical Journal Letters*, **739**  
449 (2), L62 (2011)
- 450 17. Kawahara, H. Frequency Modulation of Directly Imaged Exoplanets: Geometric Effect as a  
451 Probe of Planetary Obliquity. *The Astrophysical Journal*. **822** (2), 112 (2016).
- 452 18. Schwartz, J. C., Sekowski, C., Haggard, H. M., Pallé, E., Cowan, N. B. 2016. Inferring planetary  
453 obliquity using rotational and orbital photometry. *Monthly Notices of the Royal Astronomical*  
454 *Society*. **457** (1), 926-938 (2016).



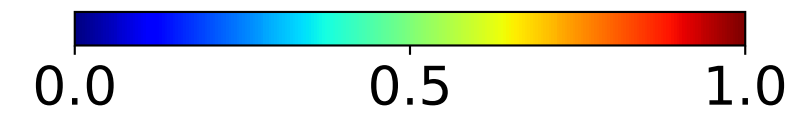
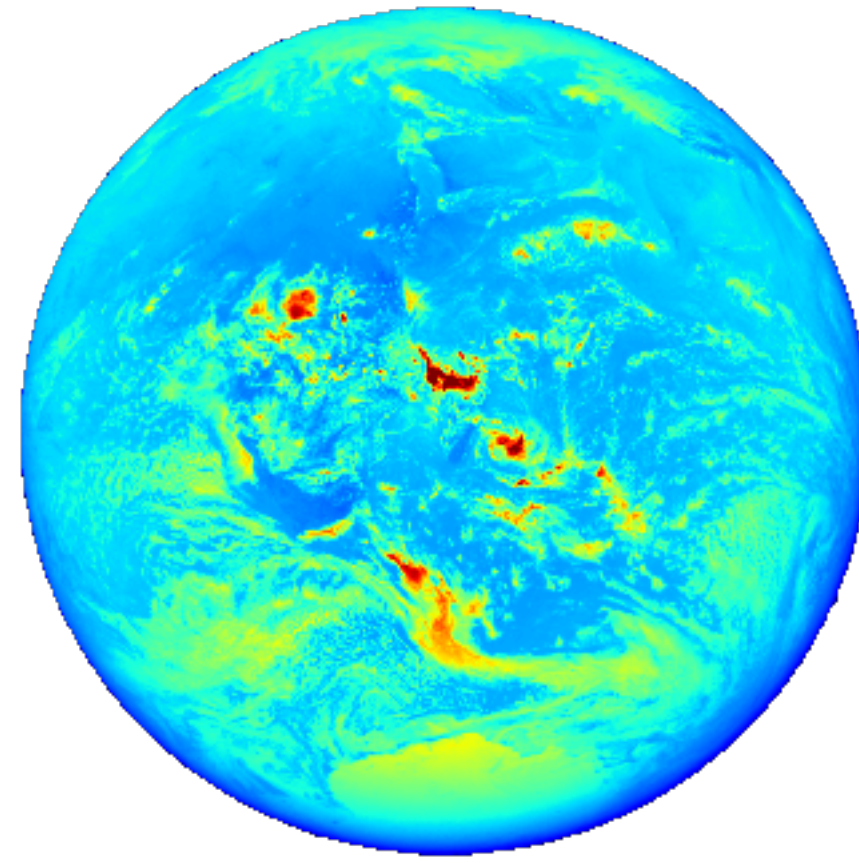
317nm



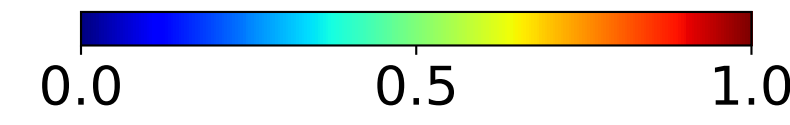
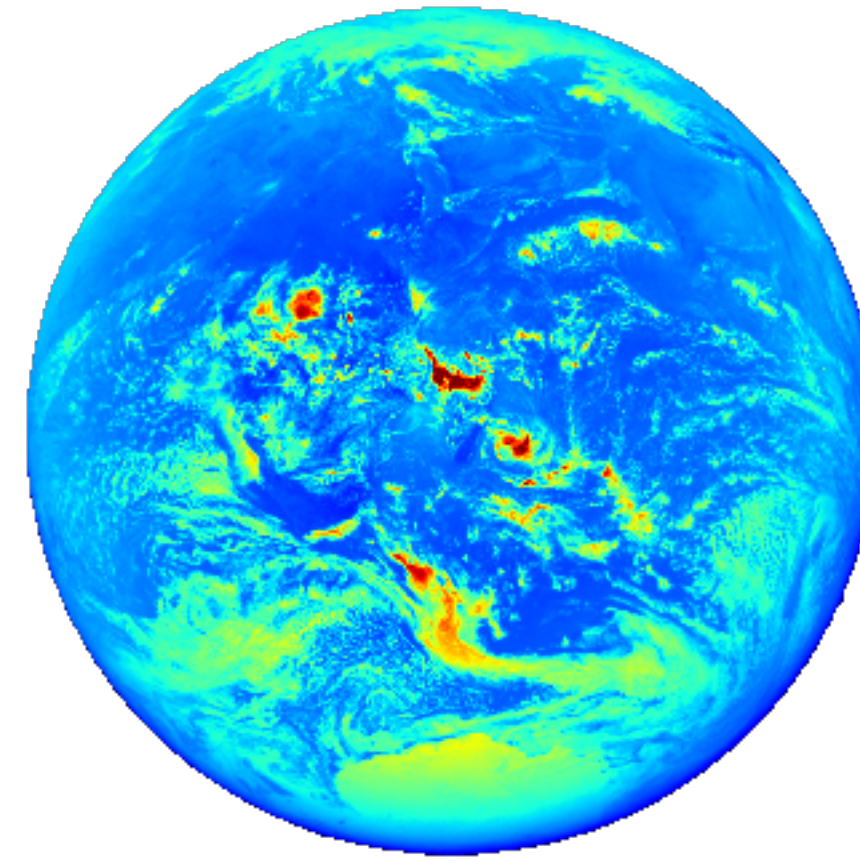
325nm



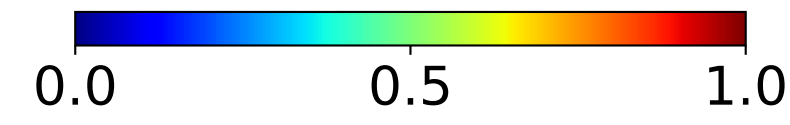
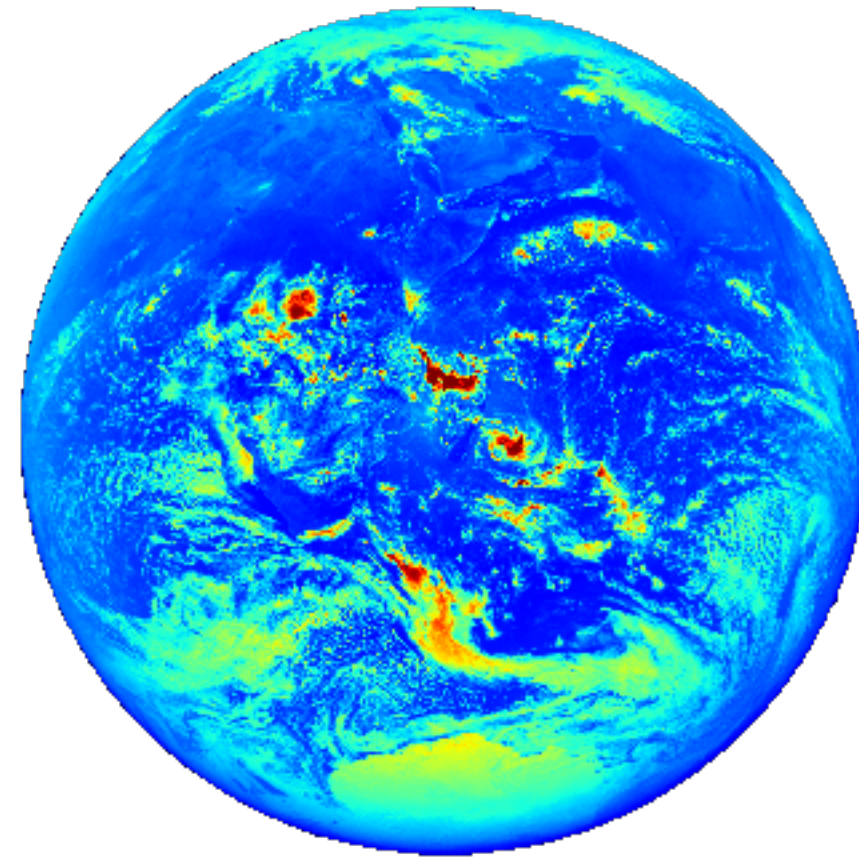
340nm



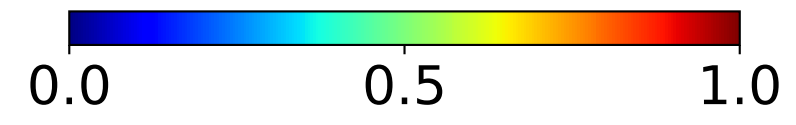
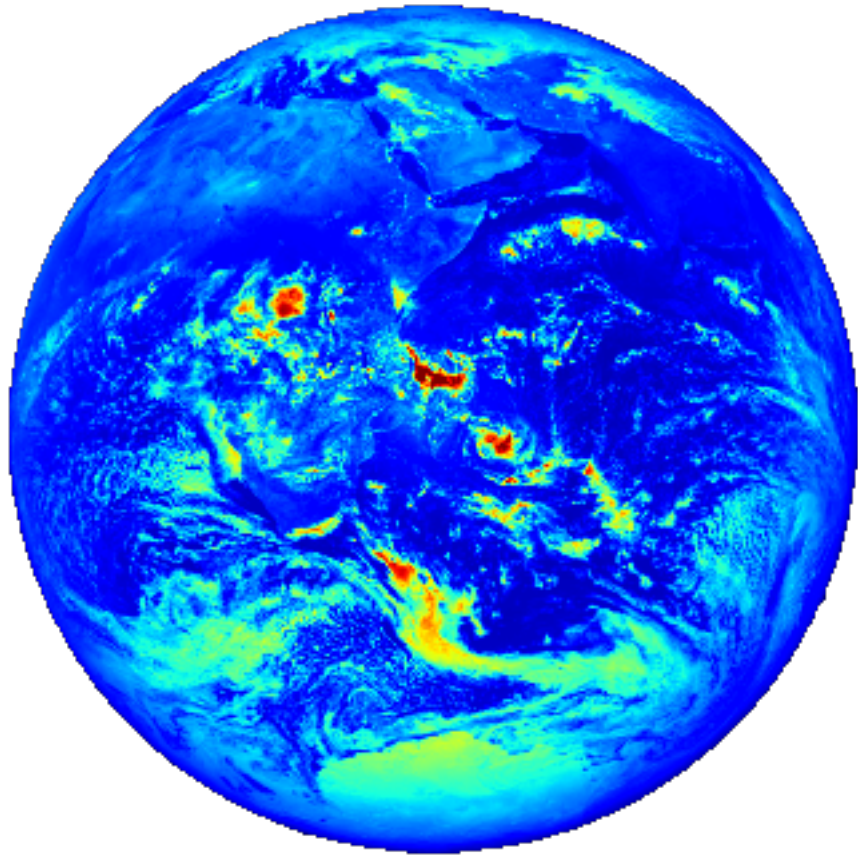
388nm



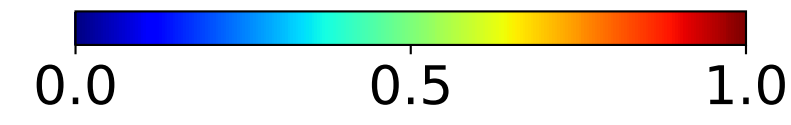
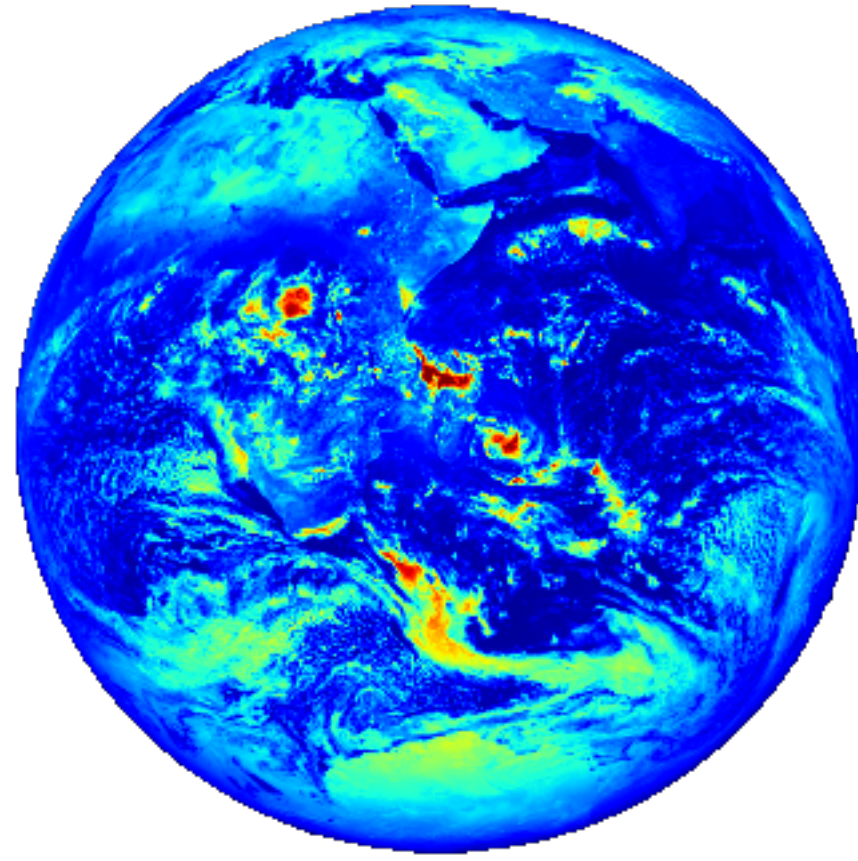
443nm



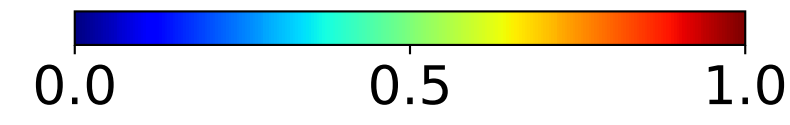
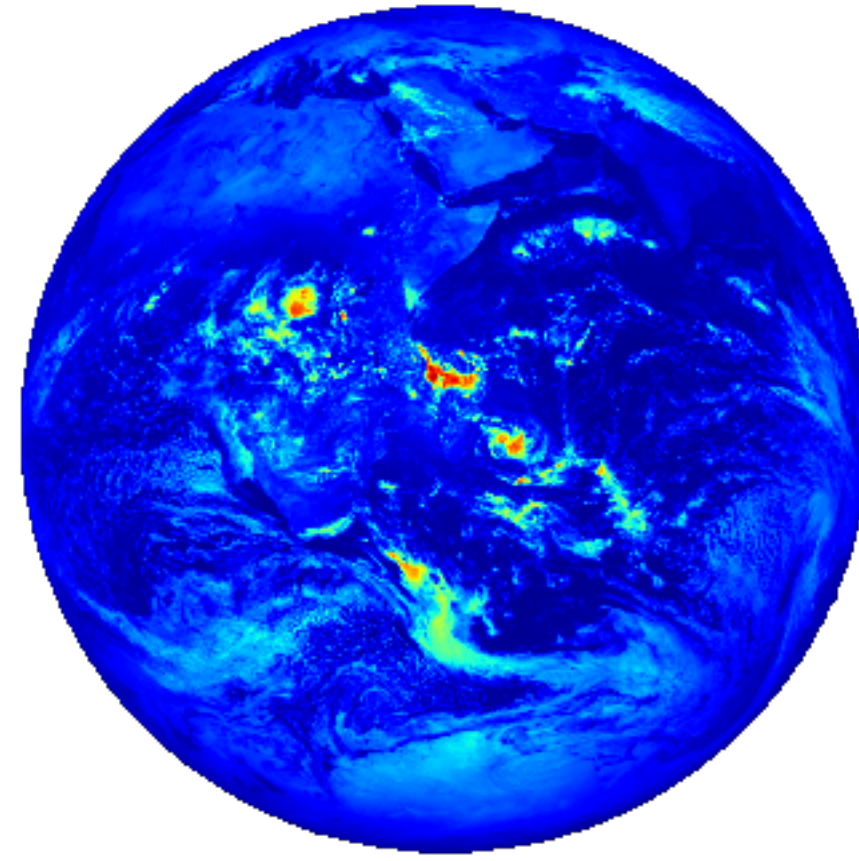
551nm



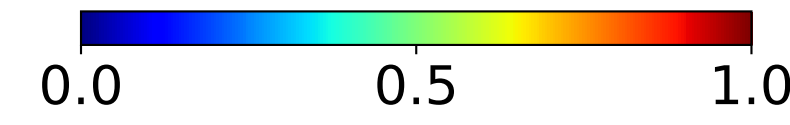
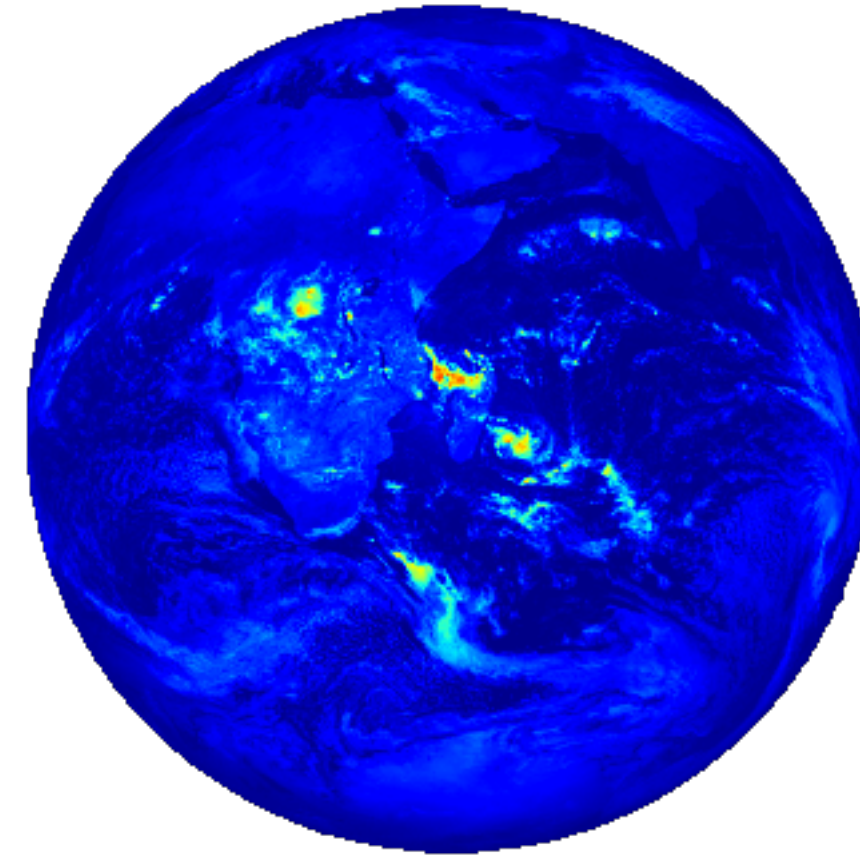
680nm



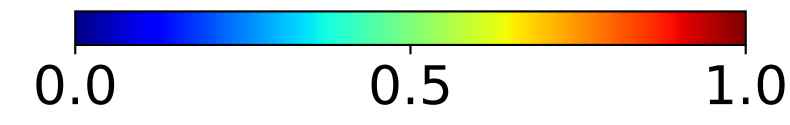
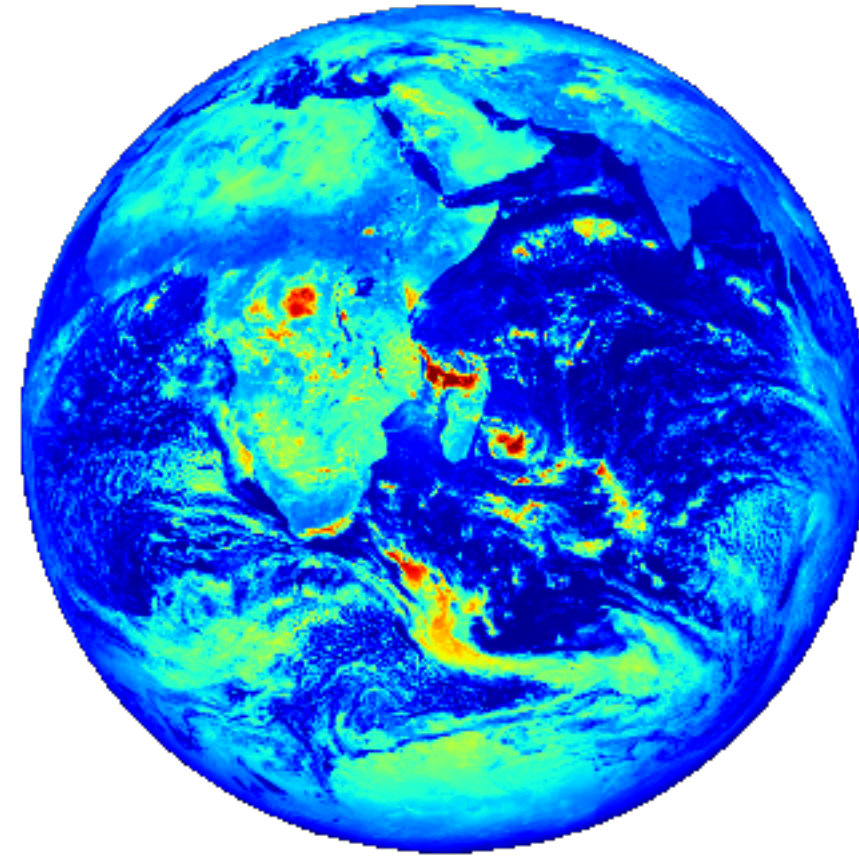
688nm



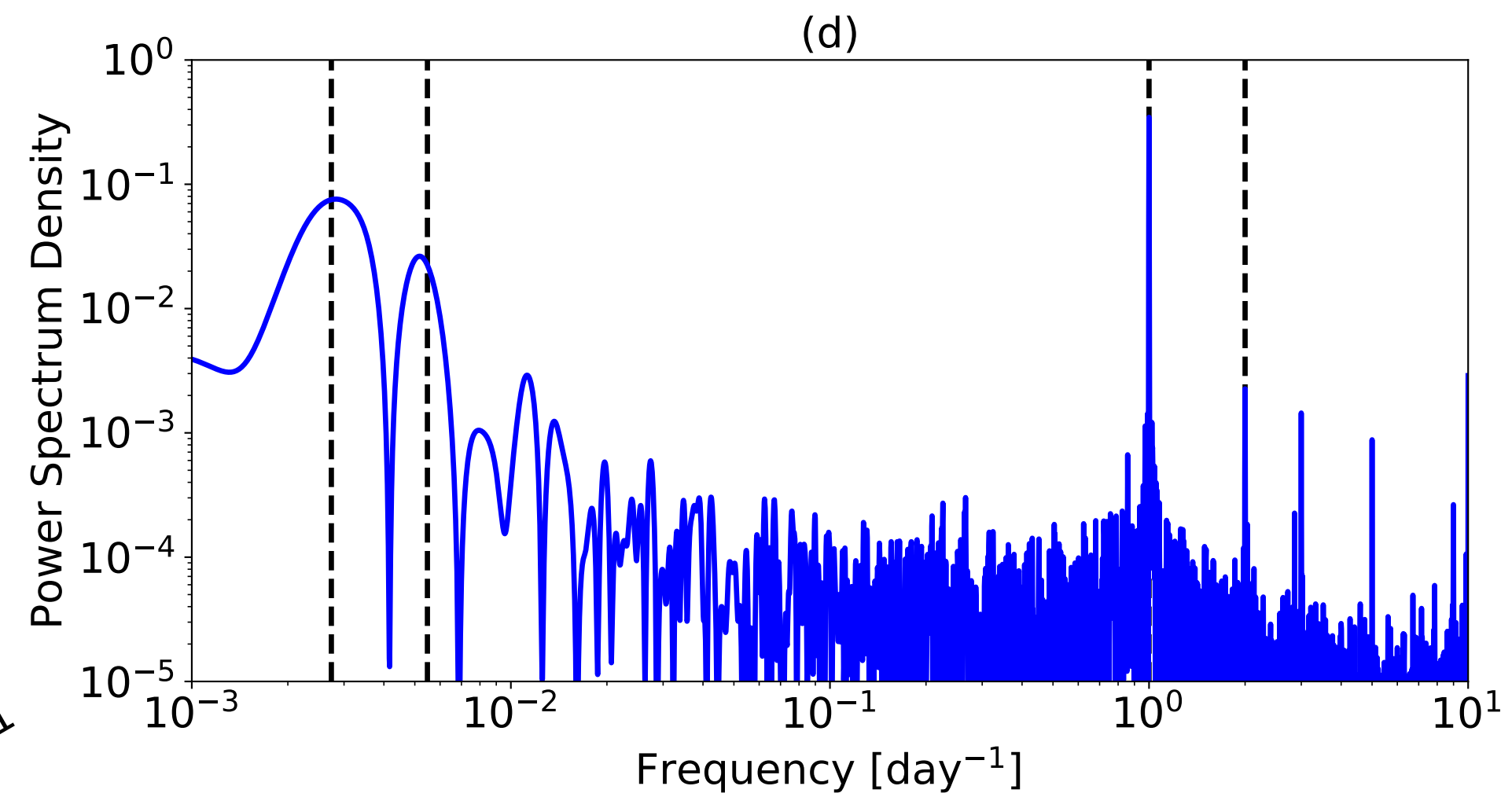
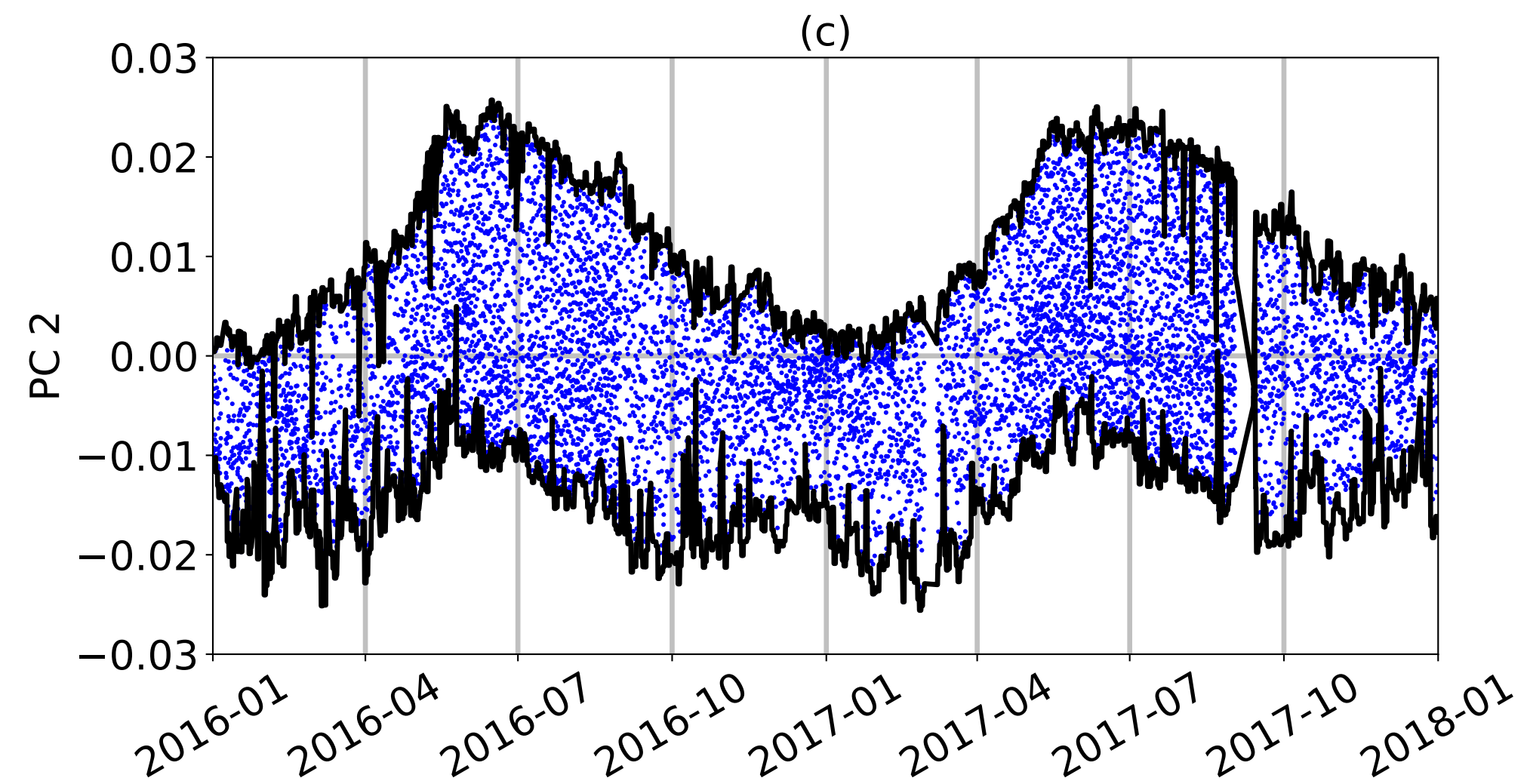
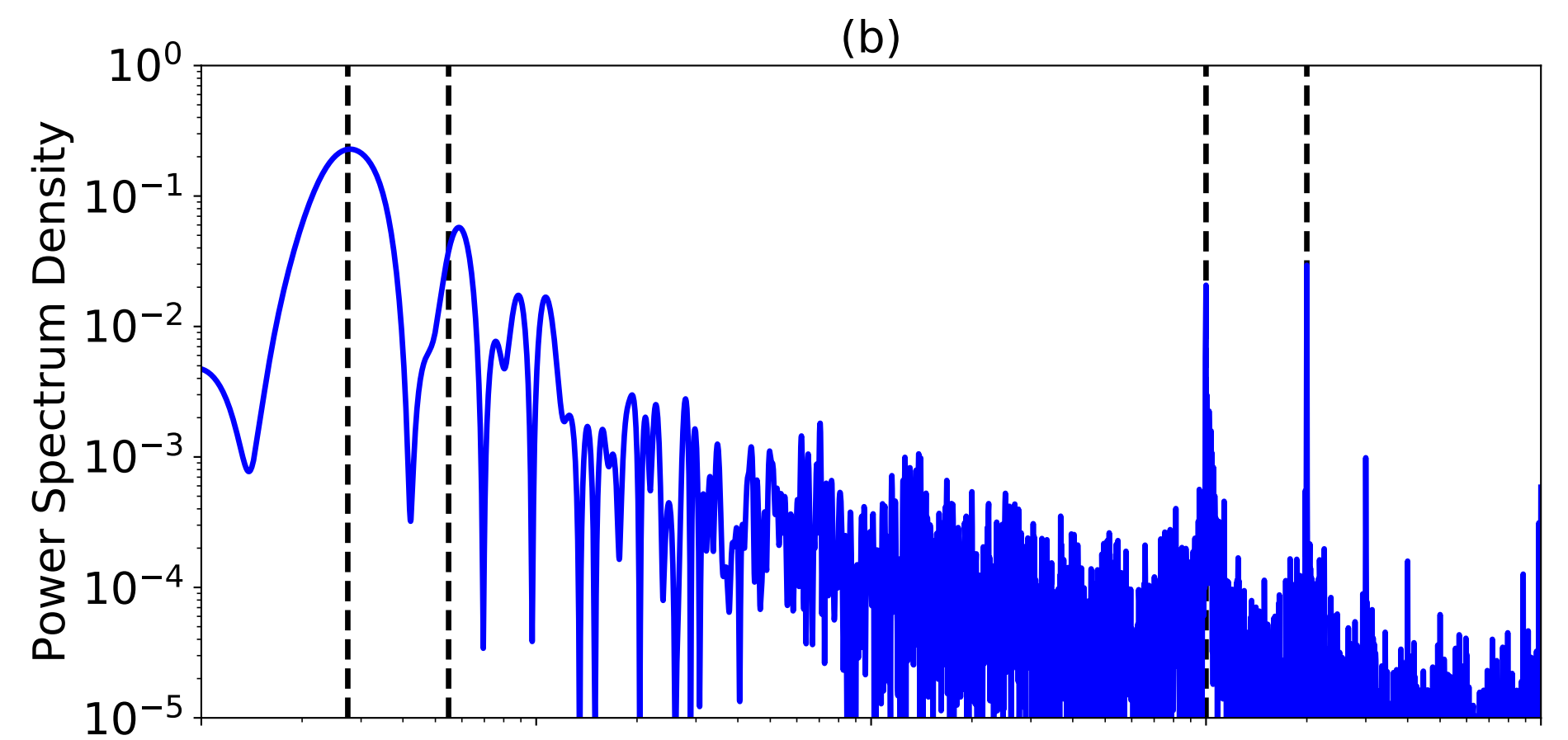
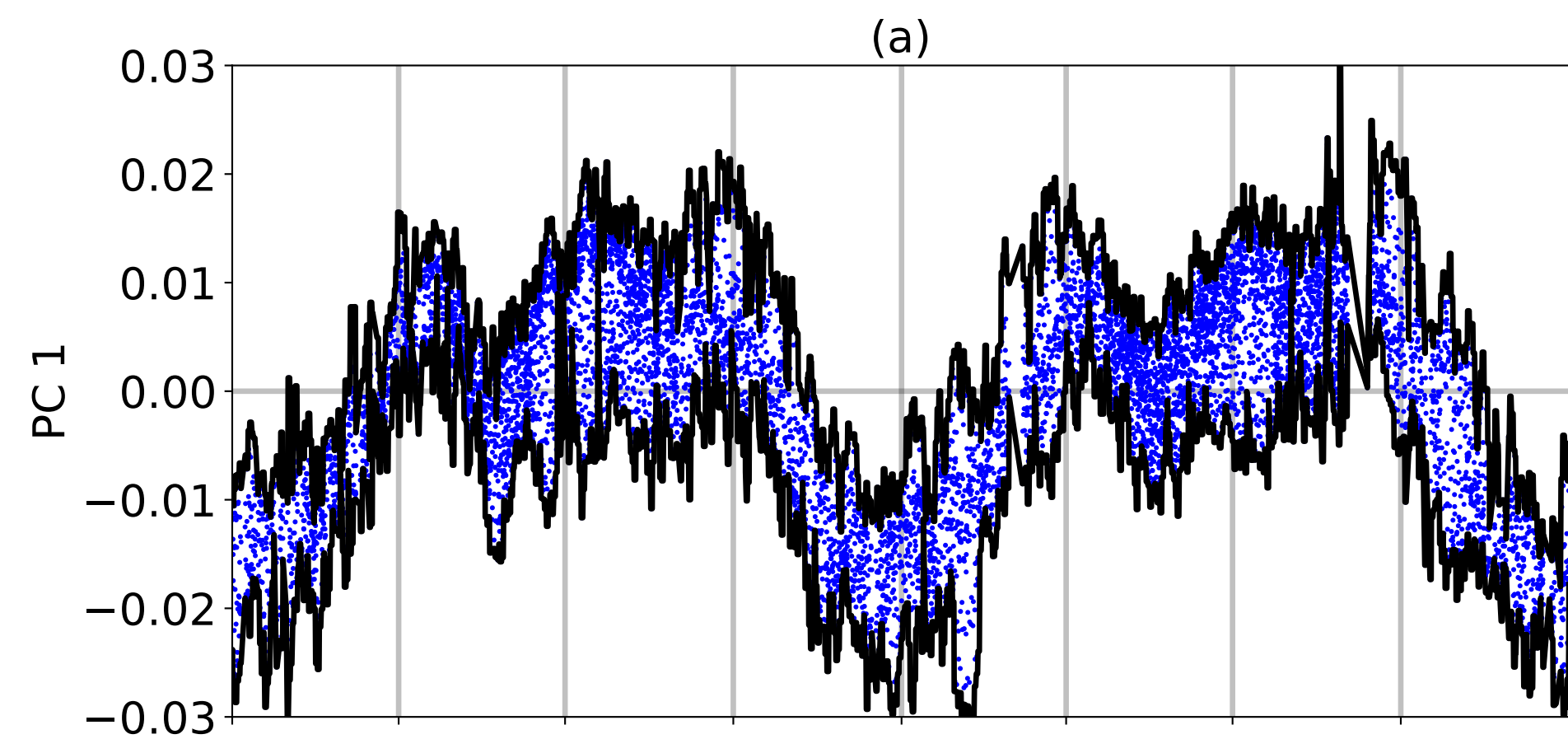
764nm



780nm







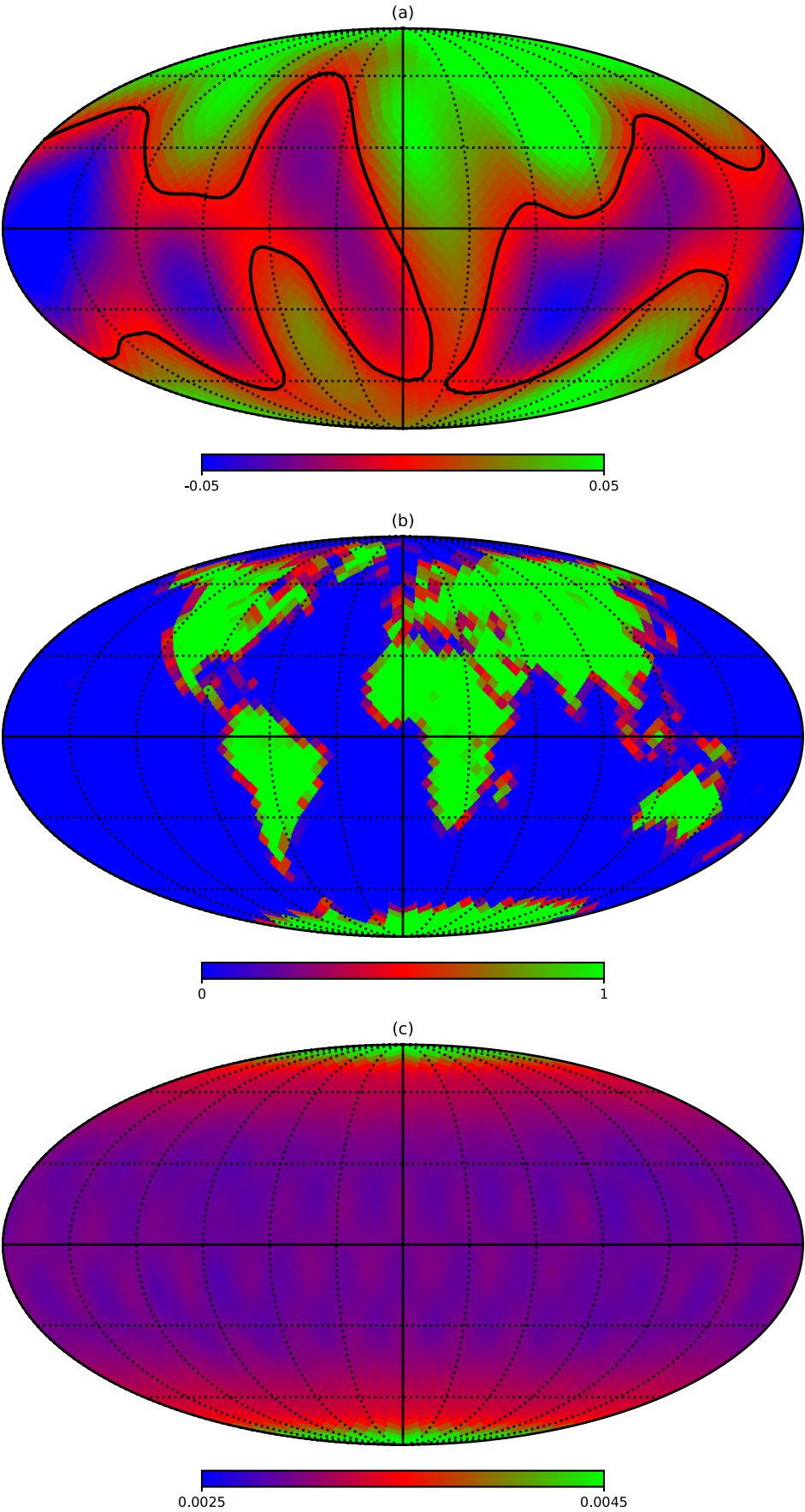


Figure 4

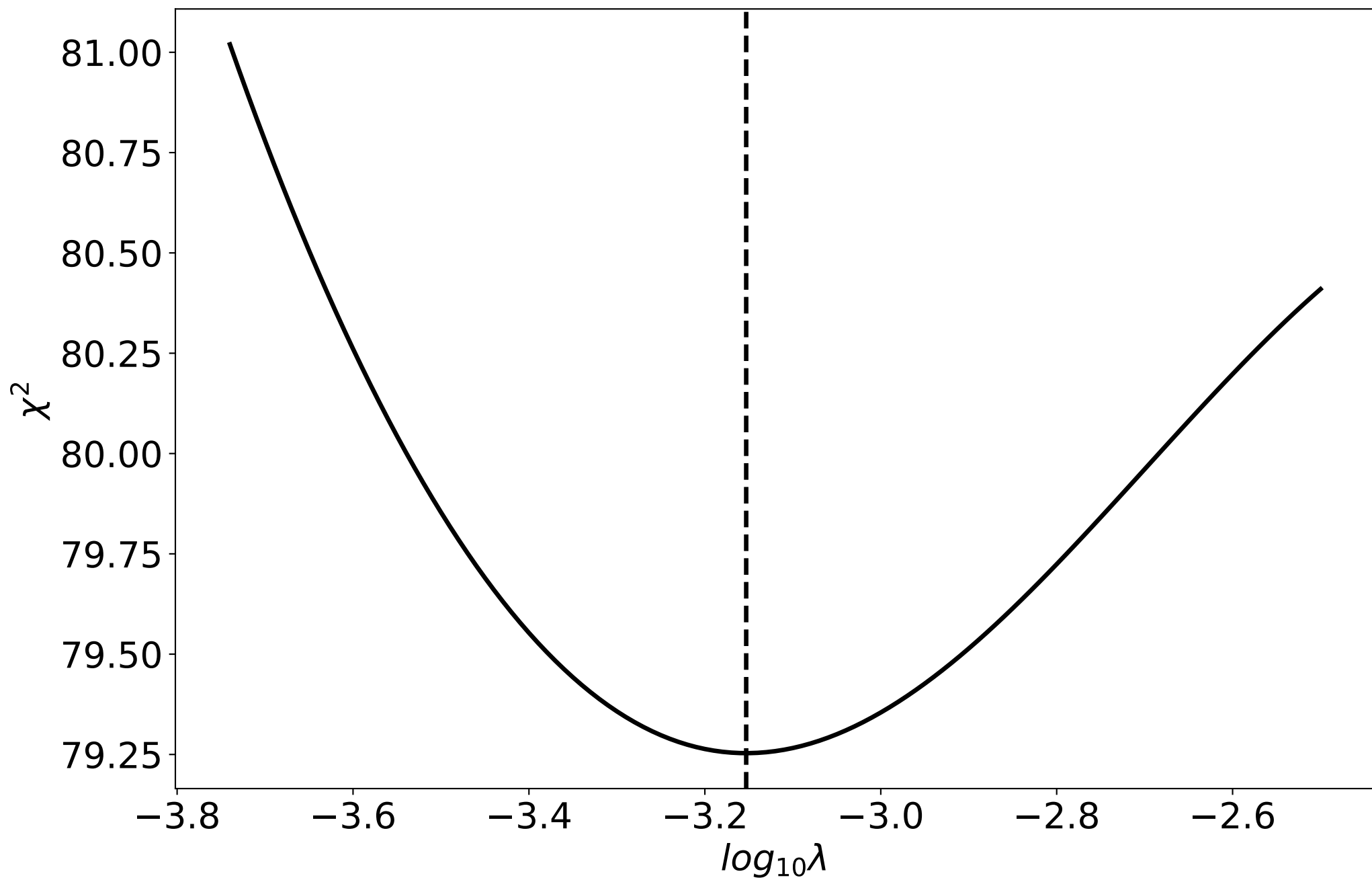
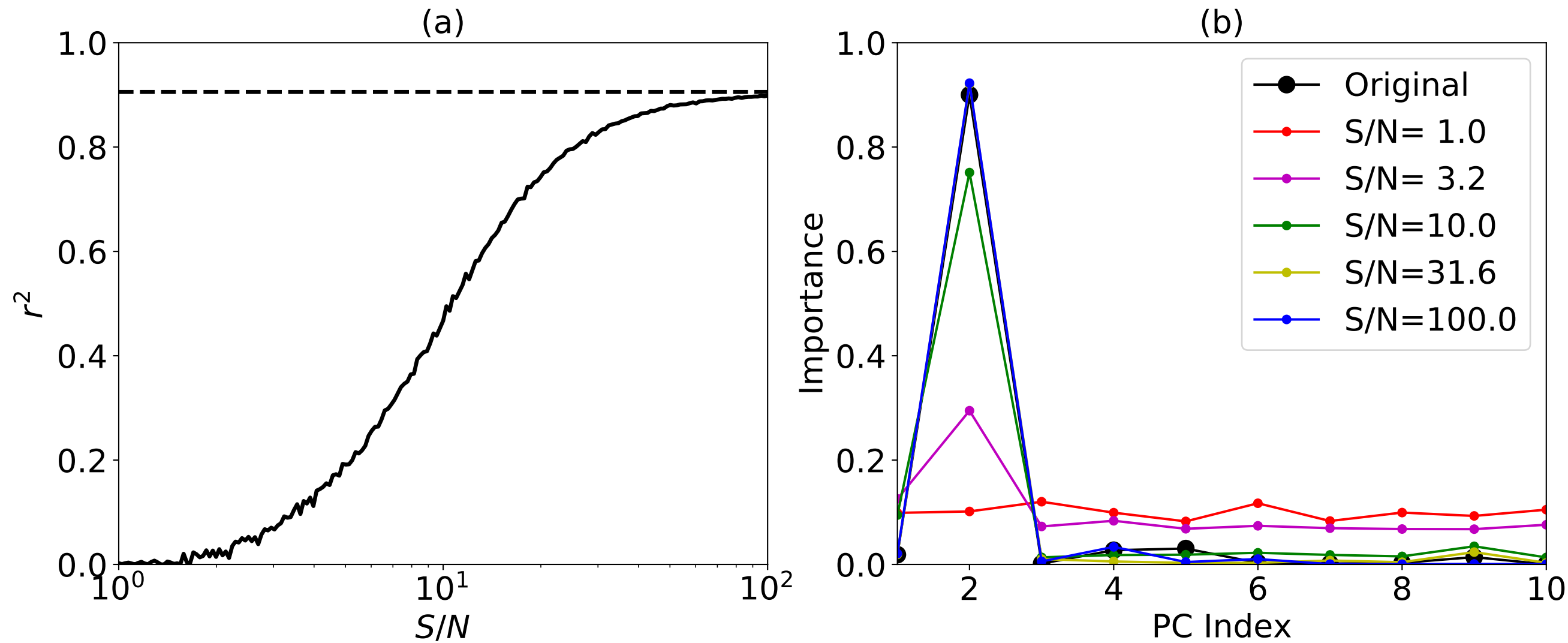


Figure 5



Name of Material/Equipment	Company	Catalog Number	Comments/Description
Python 3.7 with anaconda and healpy packages			Other programming environments (e.g., IDL or N

1ATLAB) also work.

## Rebuttal Letter

Dear Editor,

I am writing to resubmit our manuscript entitled “Surface Mapping of Earth-like Exoplanets using Single Point Light Curves” for consideration for JoVE. We greatly appreciate the editor for the efforts. We responded the comments in the manuscript and highlighted ~2.5 pages of the protocol. The changes of the manuscript are marked as blue.

As most of the protocol is mathematics, we attached the code and data with the paper. We merged the scripts to the same step where the mathematics is presented. There are plotting steps after each computing script. Windows with created figures will be displayed when running the plotting scripts, and the figures are saved as png files as well. We included what will happen at these steps so that the production team can have a better sense.

We hope that most of the filming issues are addressed this time, and are happy to address any future details if they are not clear.

Sincerely,

Siteng Fan

Division of Geological and Planetary Sciences,  
California Institute of Technology

[stfan@gps.caltech.edu](mailto:stfan@gps.caltech.edu)



Figure S1

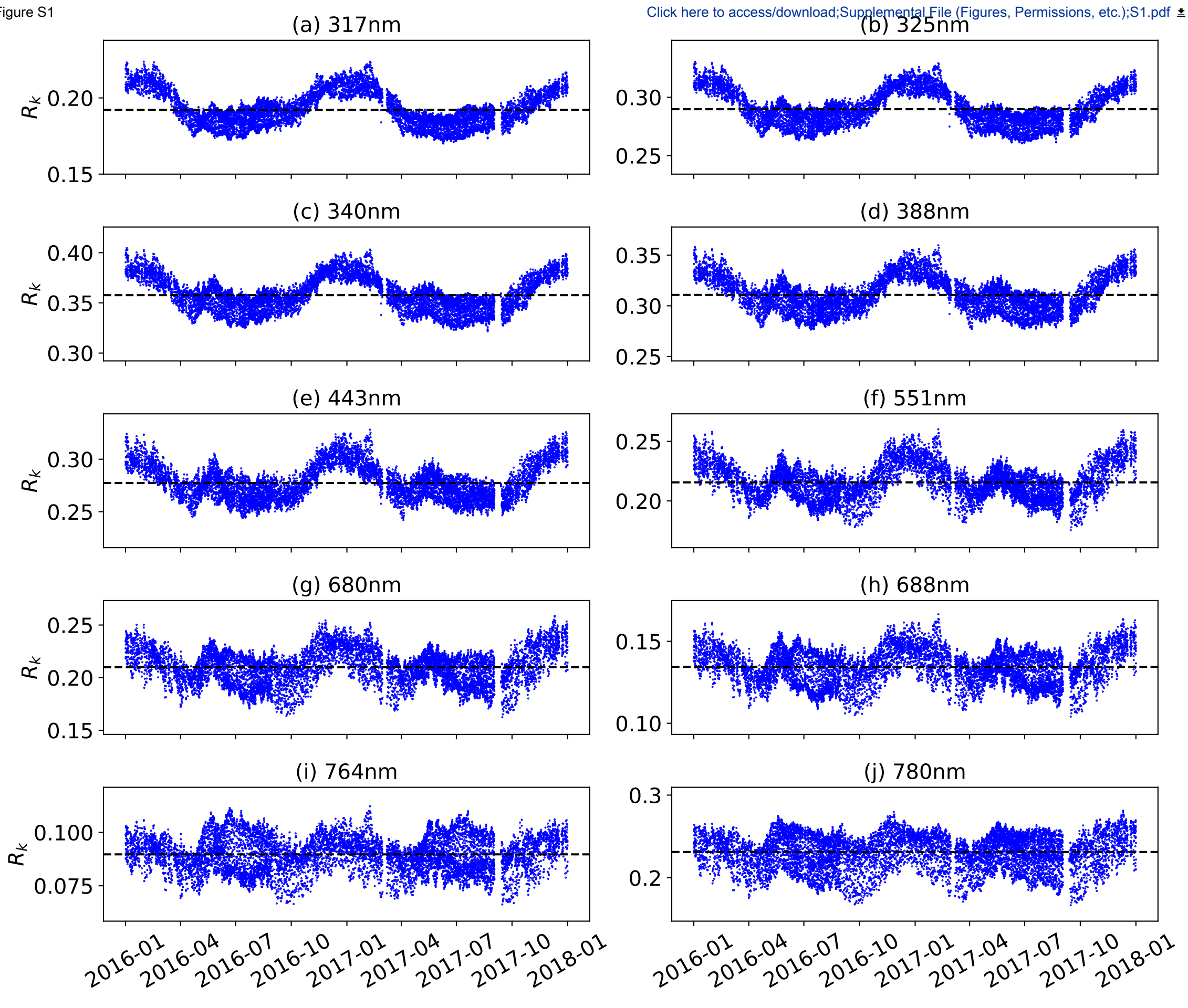
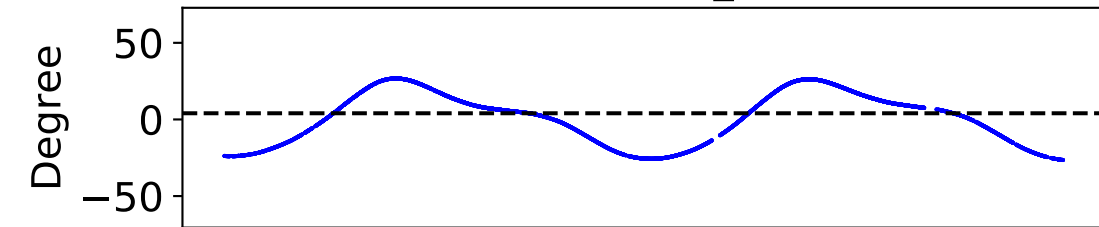
[Click here to access/download;Supplemental File \(Figures, Permissions, etc.\);S1.pdf](#)

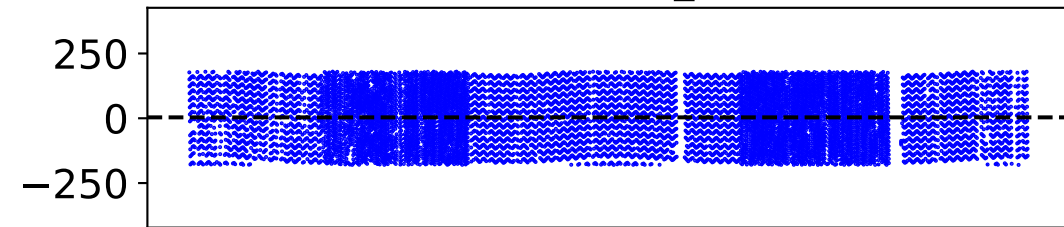
Figure S2

[Click here to access/download:Supplemental File \(Figures, Permissions, etc.\);S2.pdf](#)

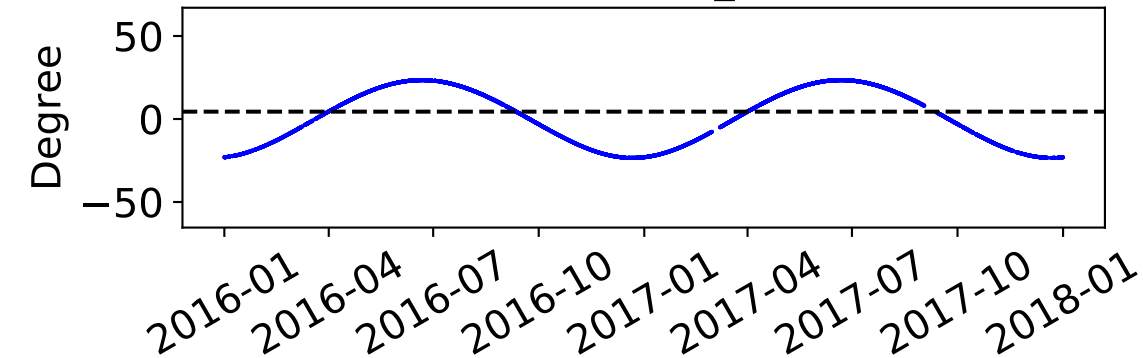
(a) SubObs\_Lat



(b) SubObs\_Lon



(c) SubStar\_Lat



(d) SubStar\_Lon

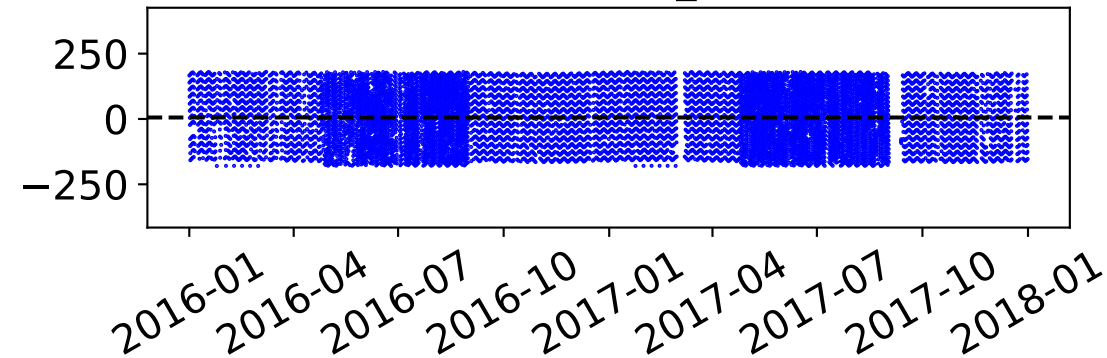


Figure S3

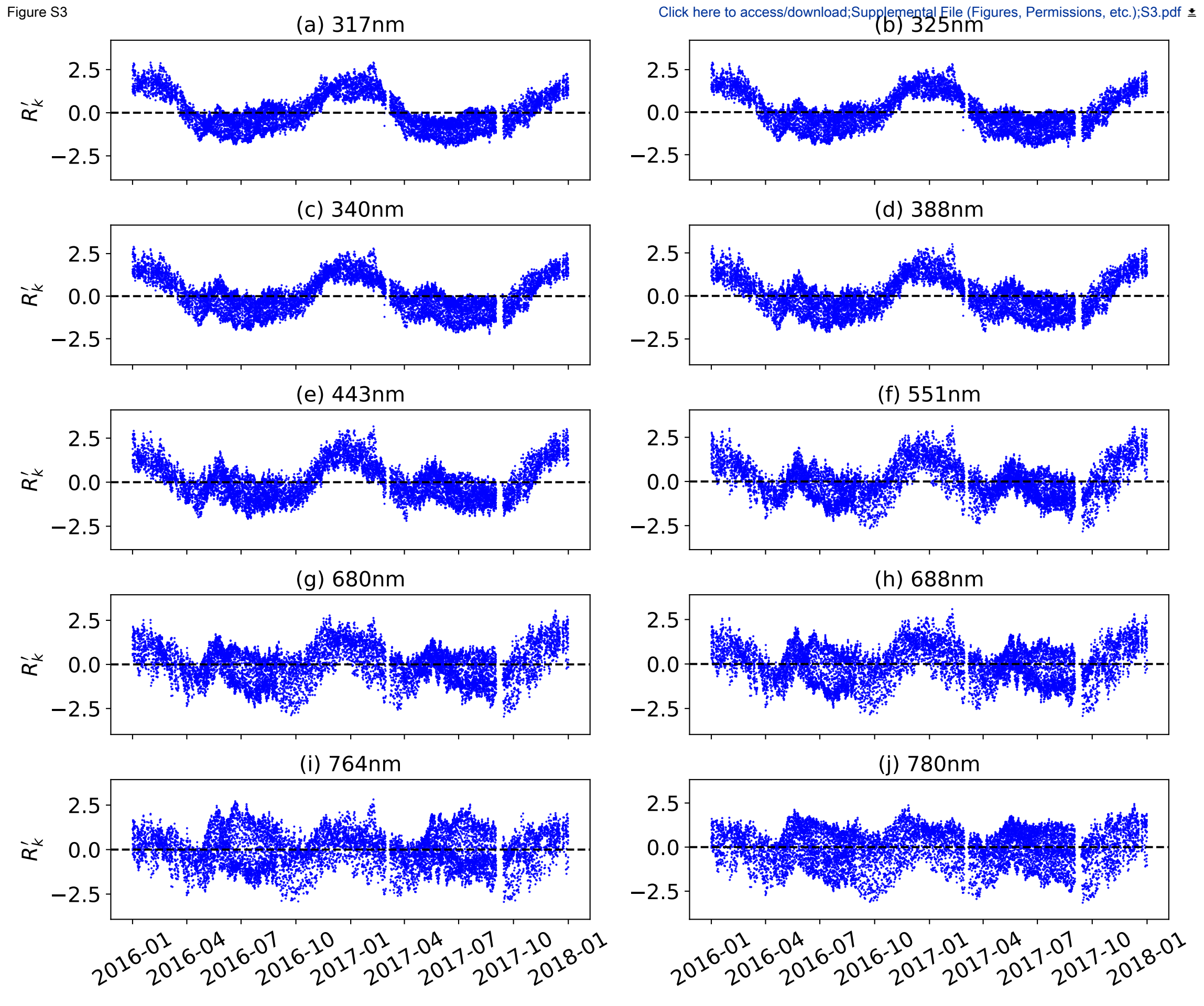
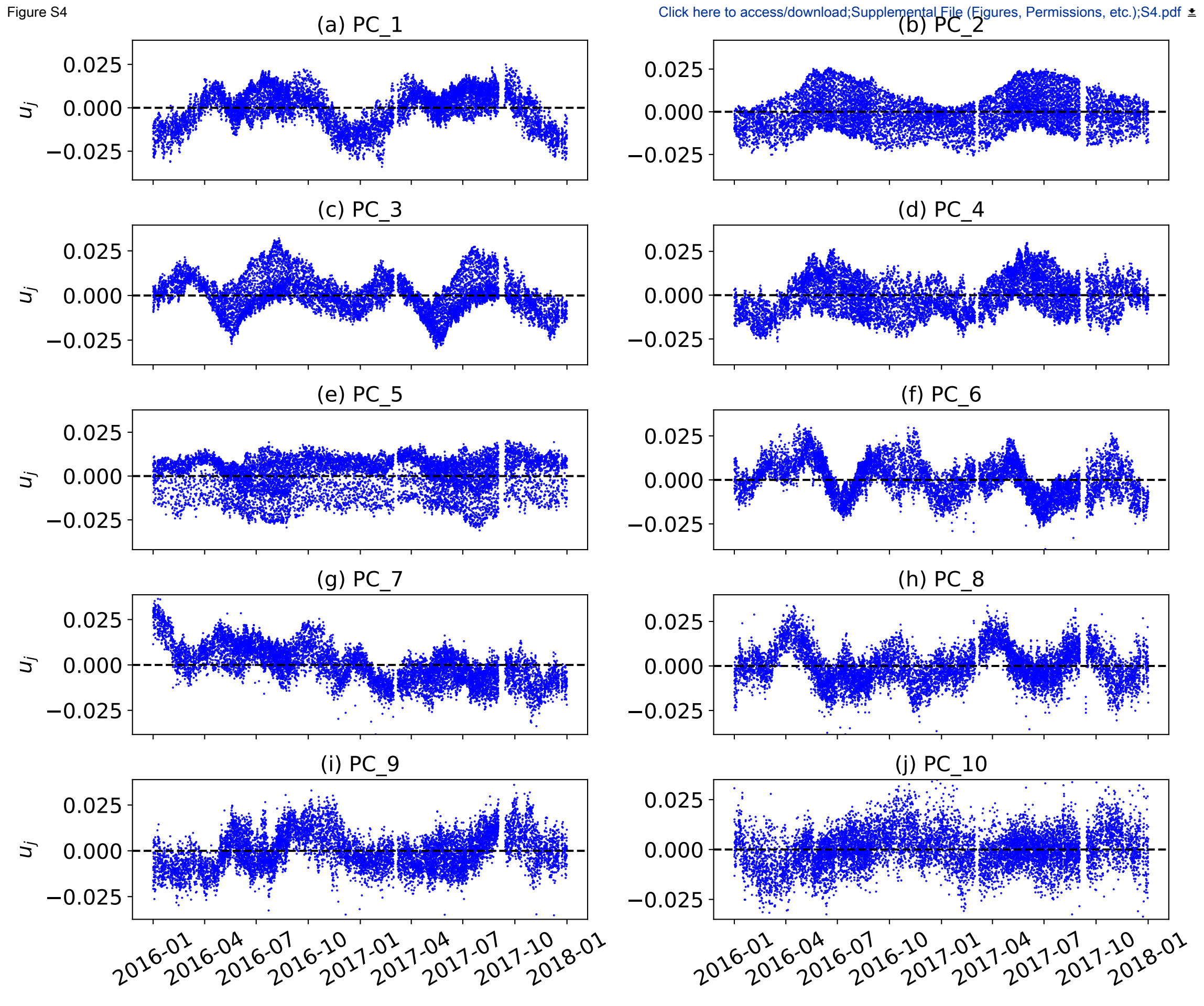
[Click here to access/download;Supplemental File \(Figures, Permissions, etc.\);S3.pdf](#)

Figure S4

[Click here to access/download;Supplemental File \(Figures, Permissions, etc.\);S4.pdf](#)

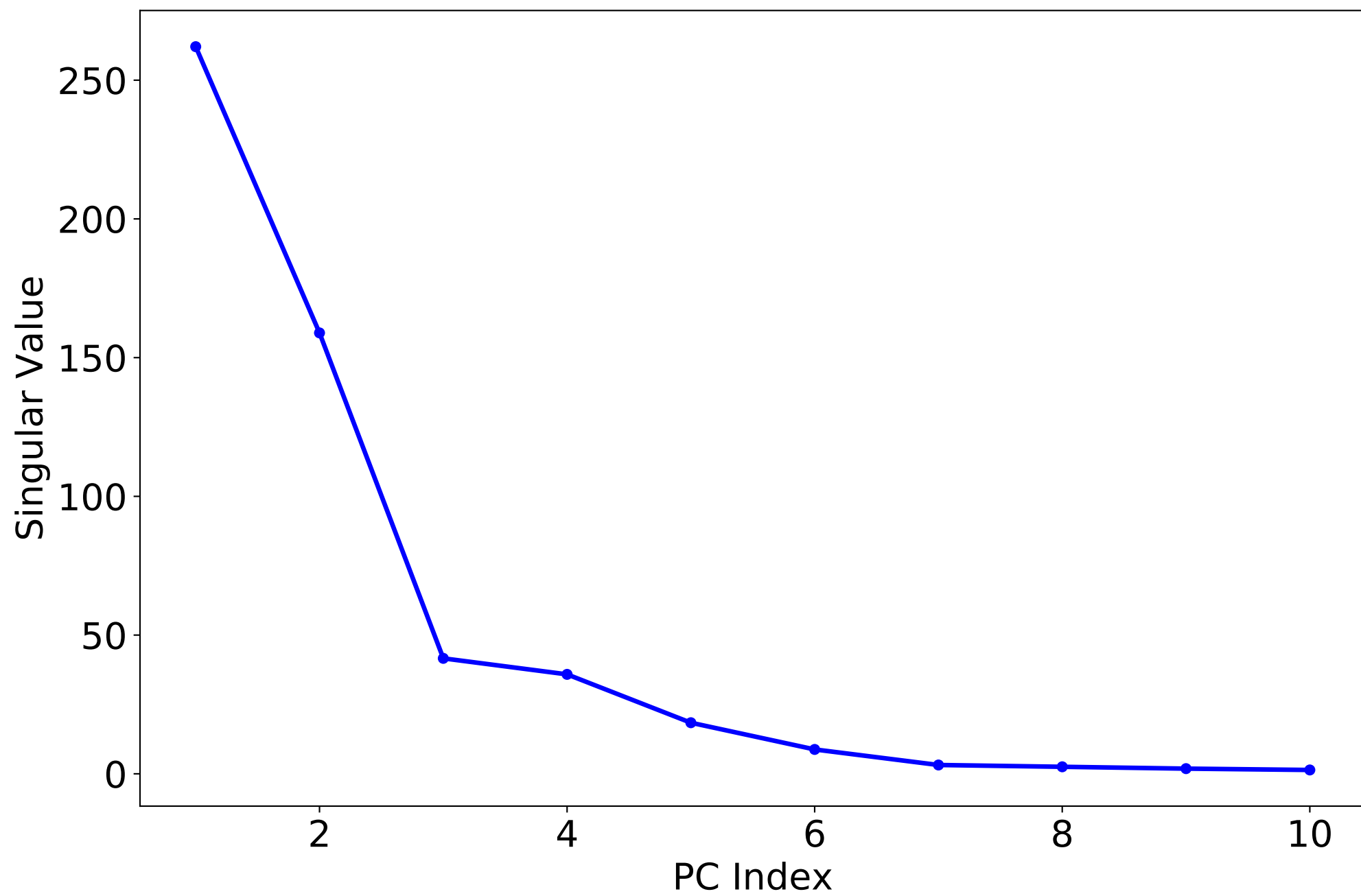


Figure S6

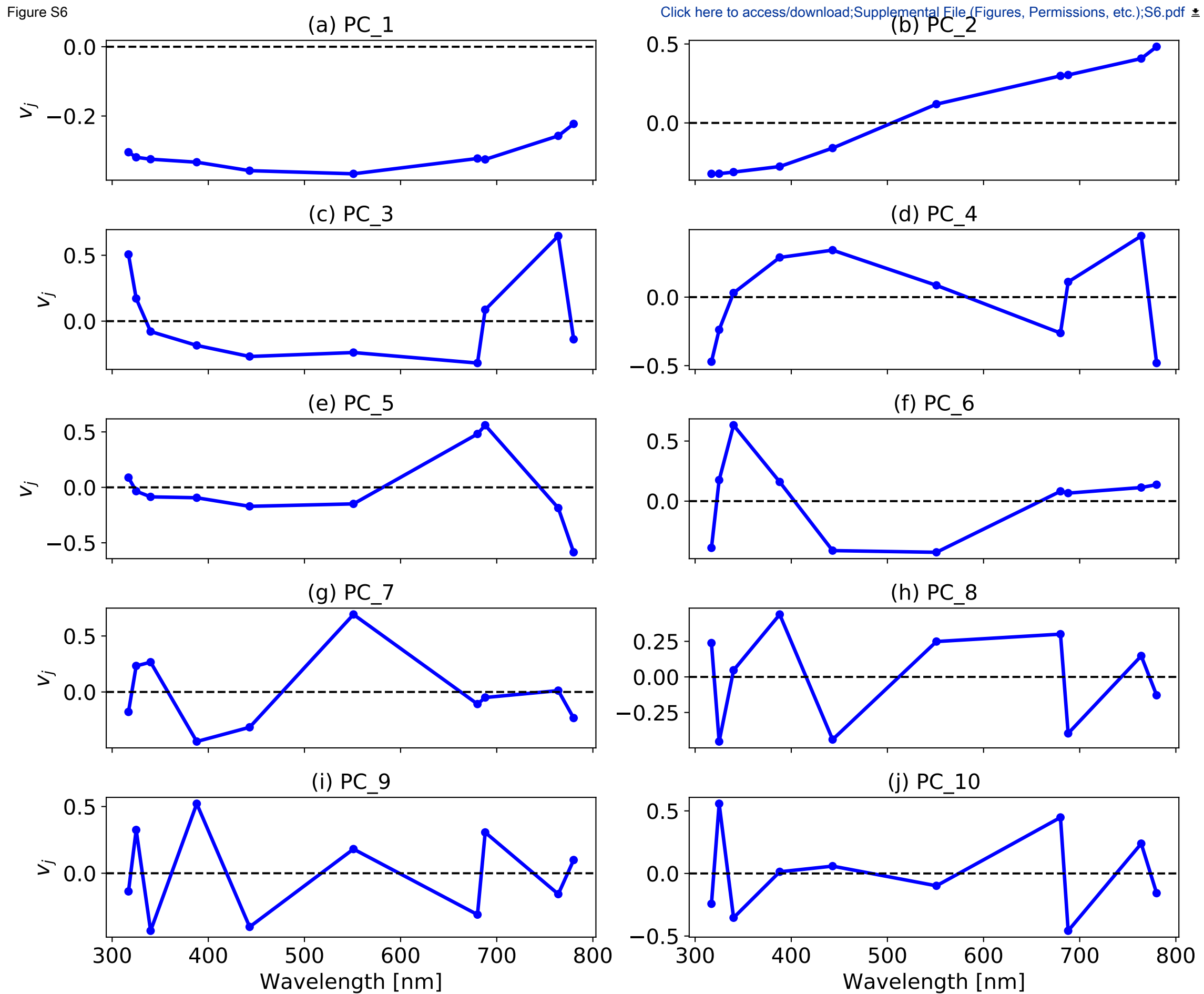
[Click here to access/download;Supplemental File \(Figures, Permissions, etc.\);S6.pdf](#)



Figure S7

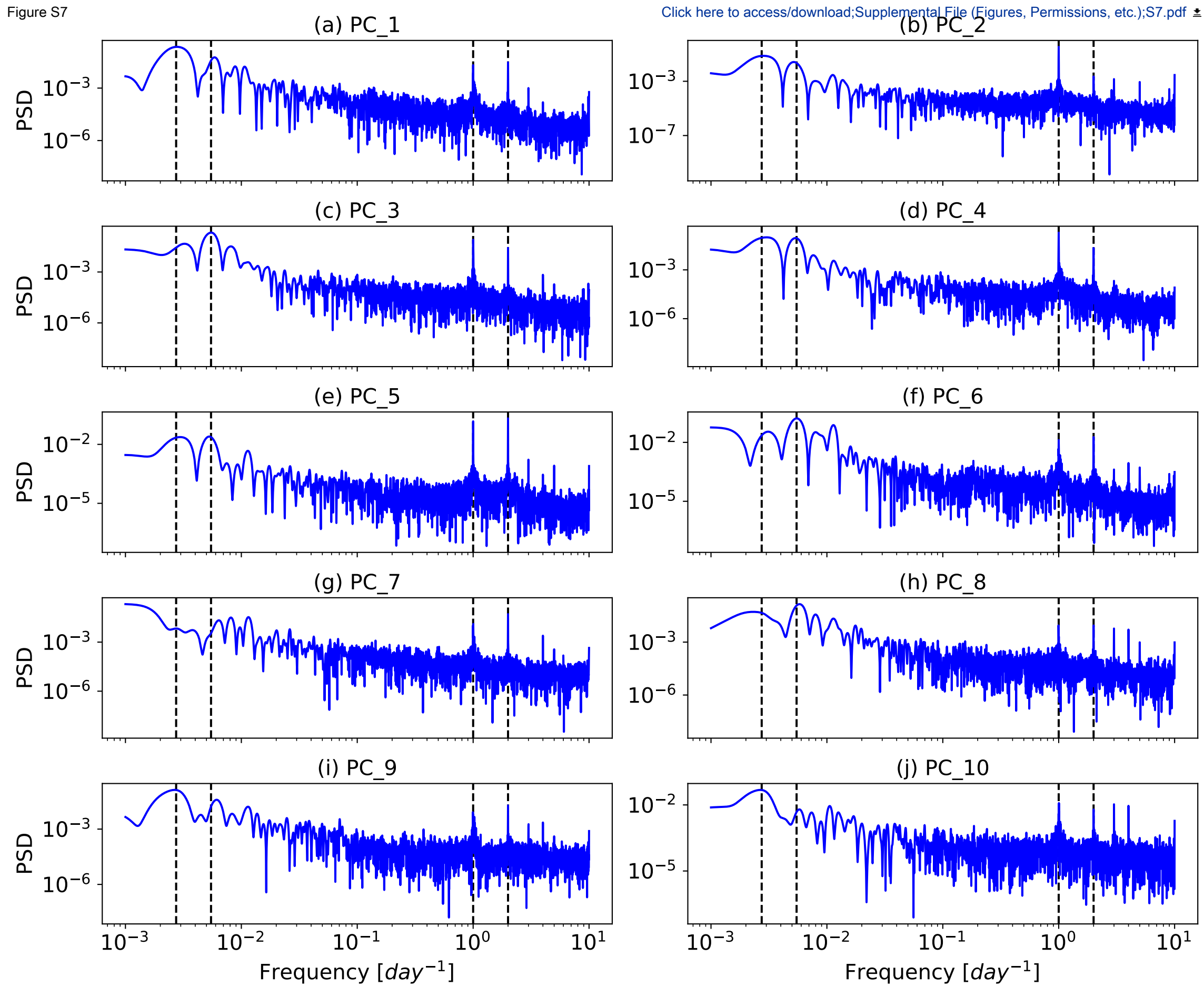
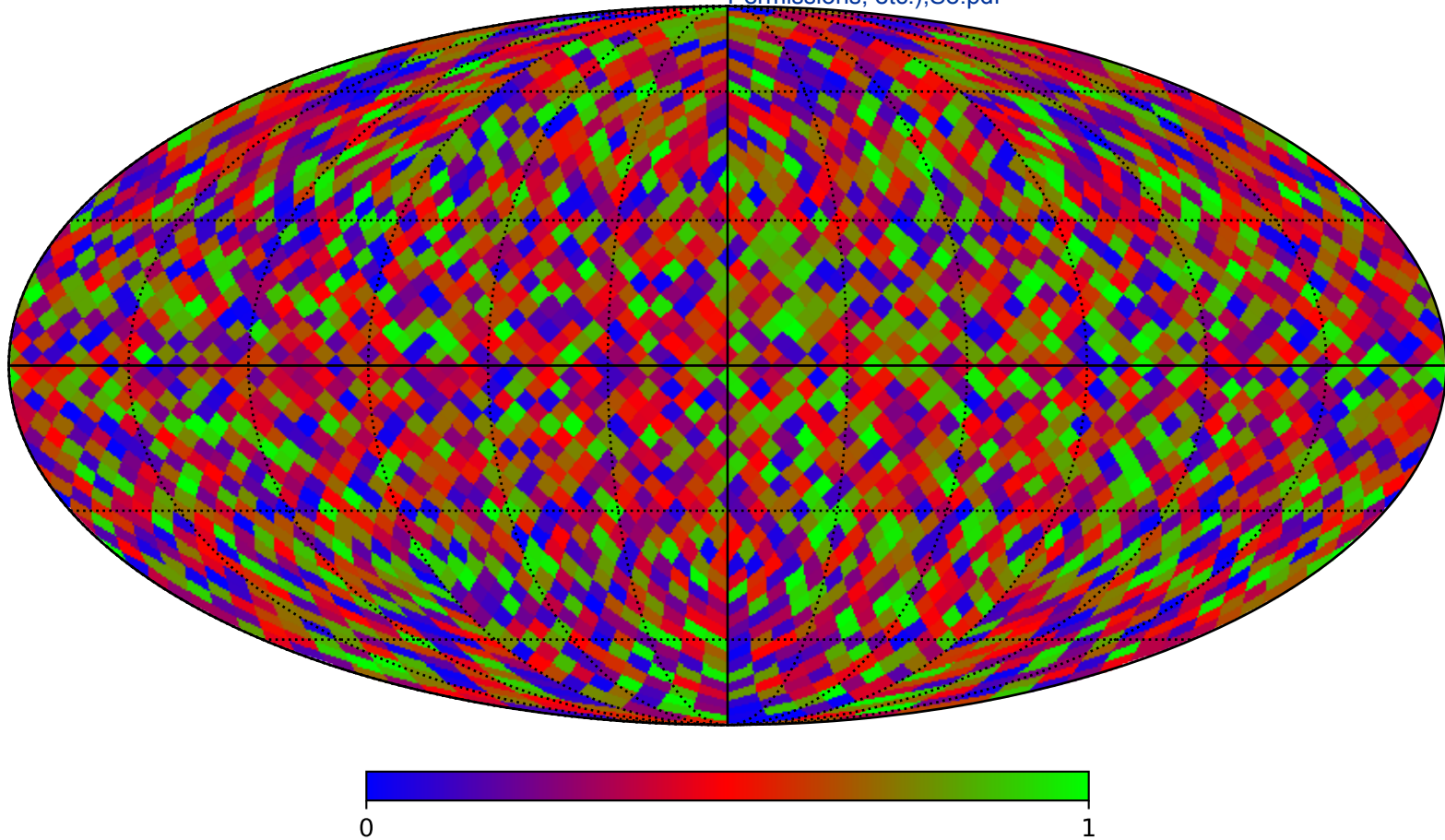
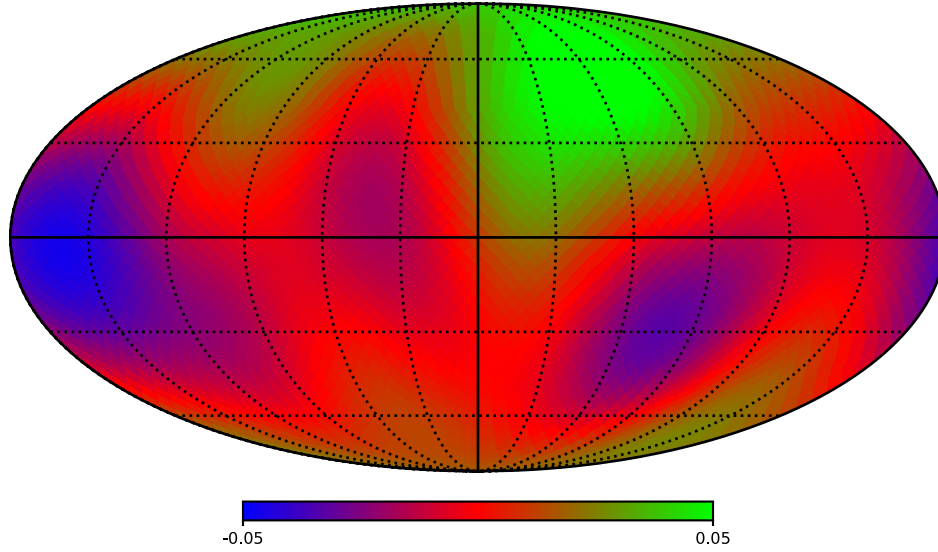
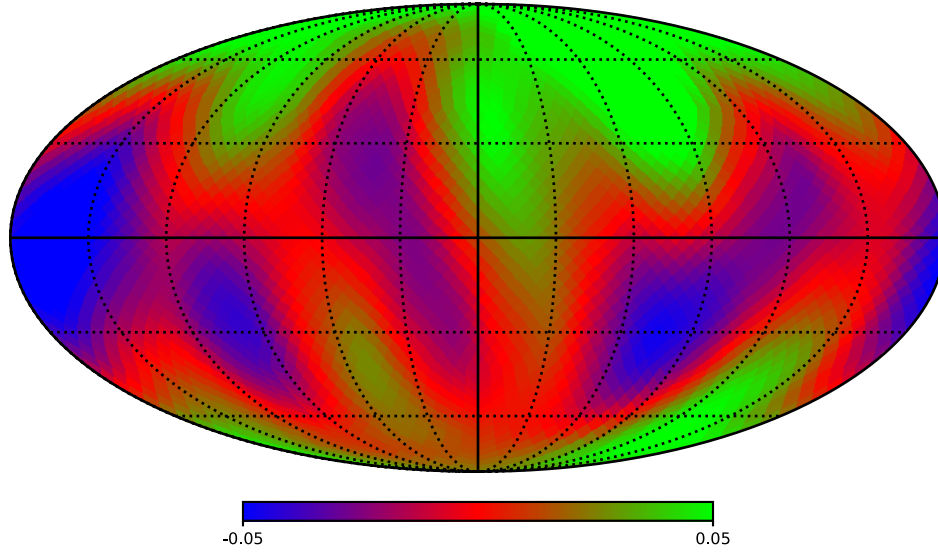
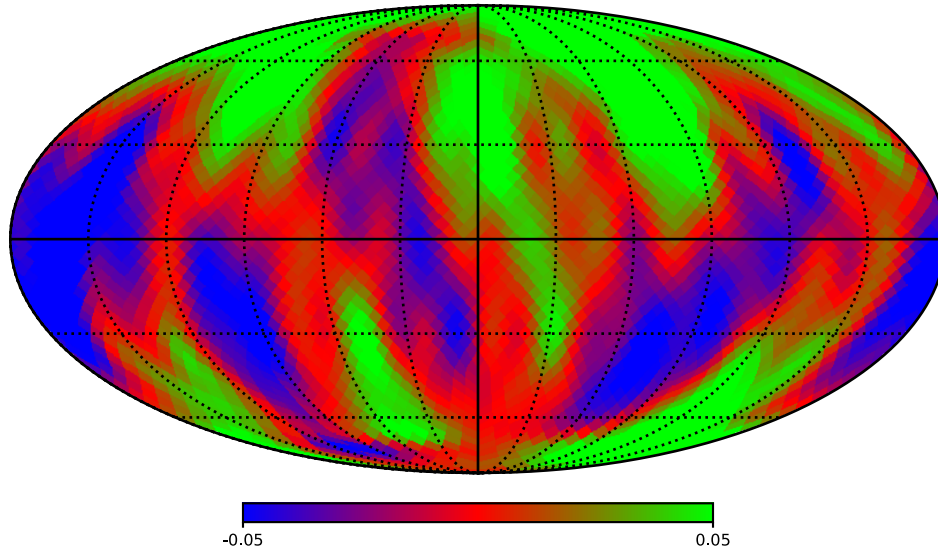
[Click here to access/download;Supplemental File \(Figures, Permissions, etc.\);S7.pdf](#)

Figure S8

Pixelization  
[Click here to access/download;Supplemental File \(Figures, Permissions, etc.\);S8.pdf](#)





(a)  $\lambda = 10^{-2}$ (b)  $\lambda = 10^{-3}$ (c)  $\lambda = 10^{-4}$ 



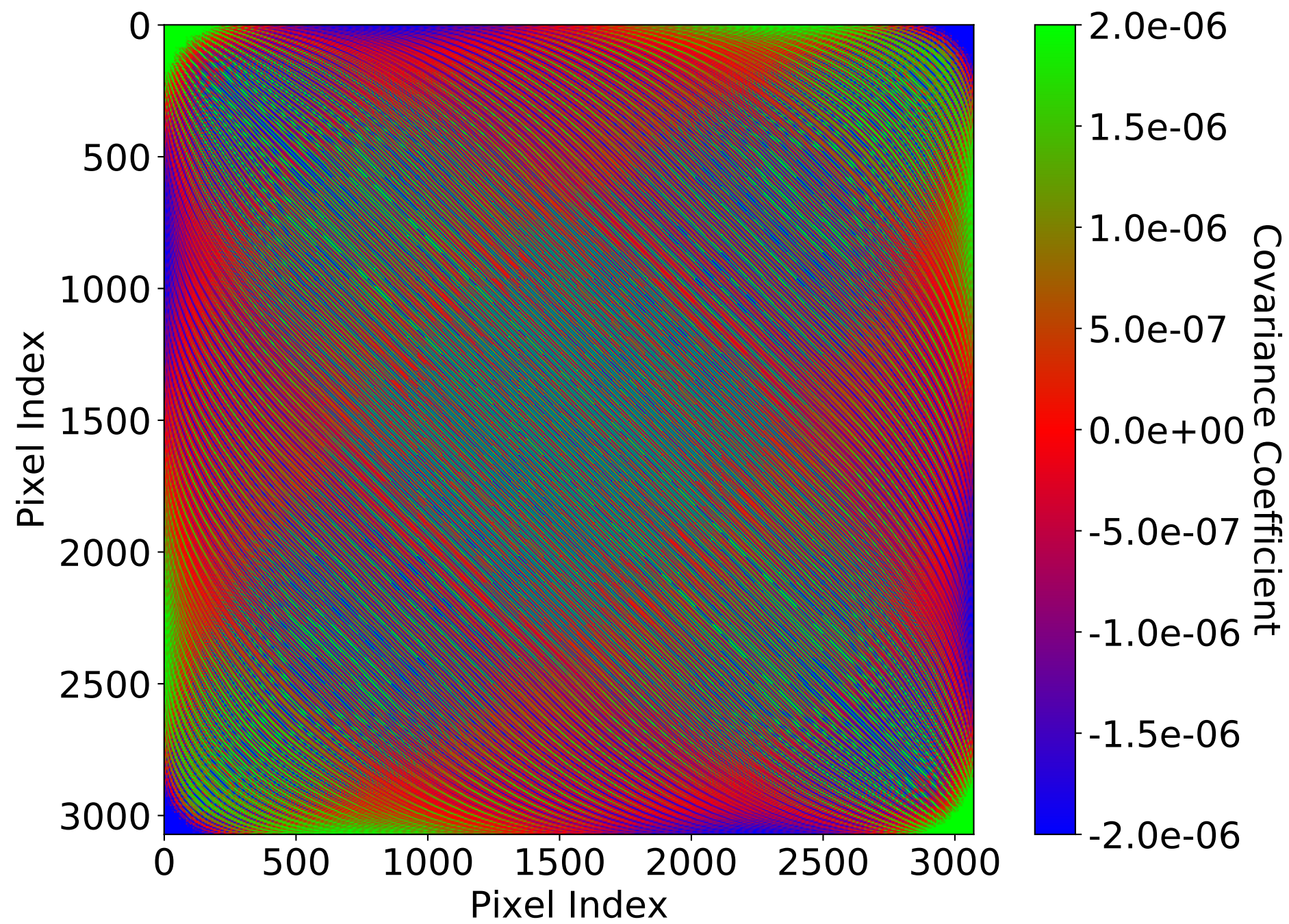
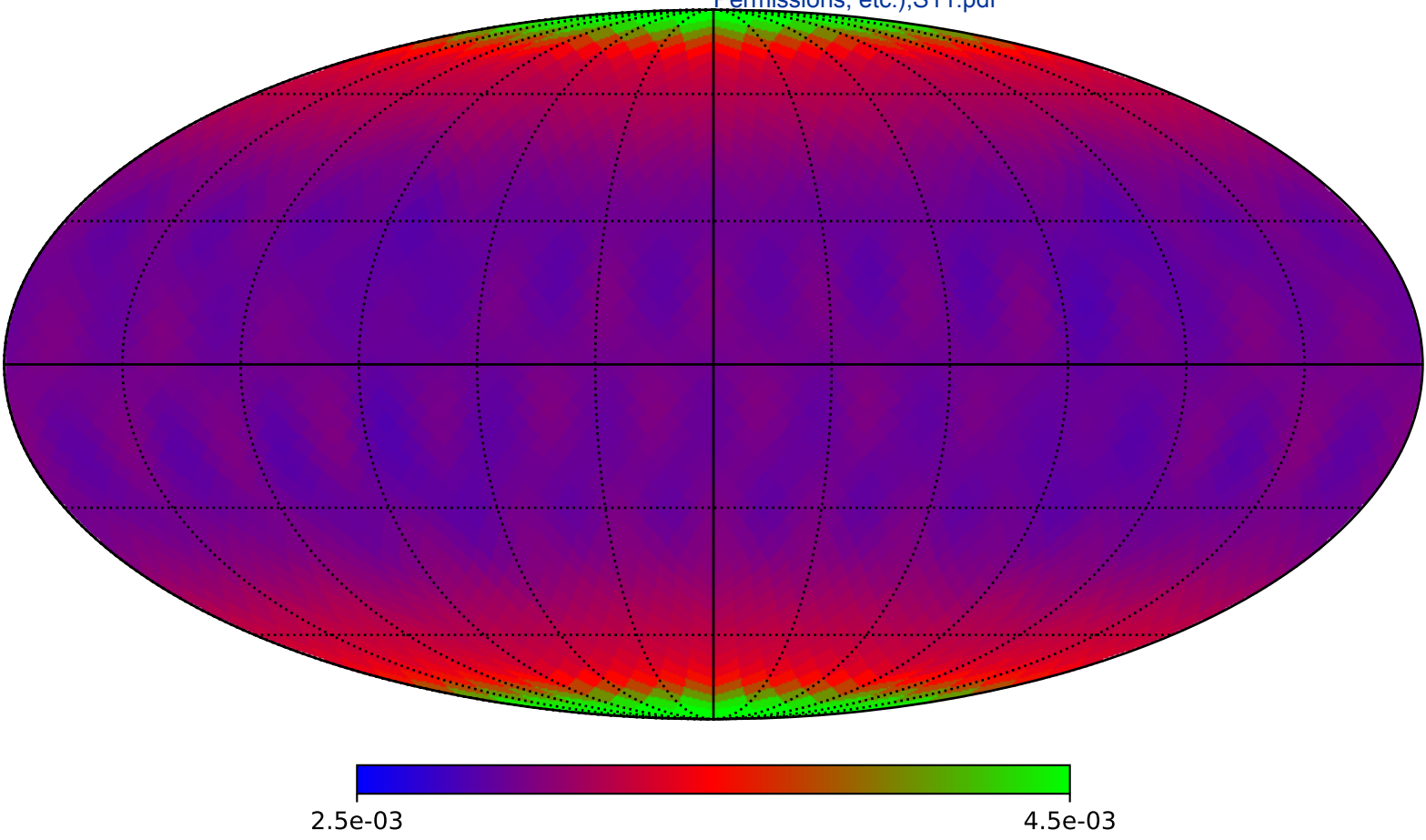
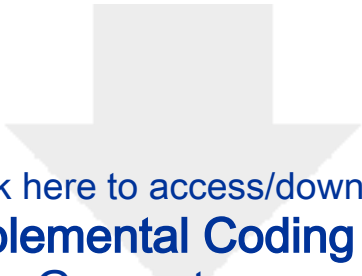


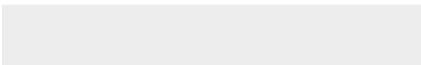
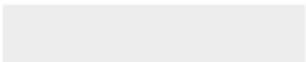


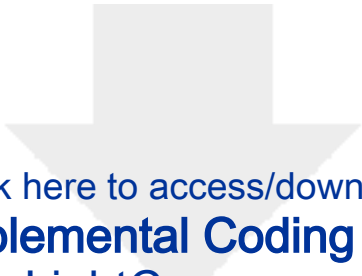
Figure S11



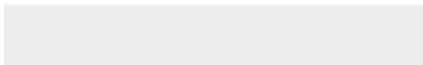


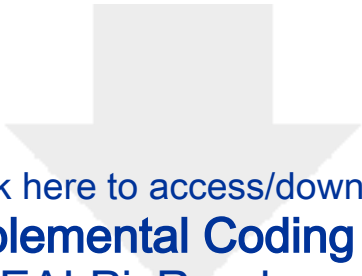
Click here to access/download  
**Supplemental Coding Files**  
Geometry.csv



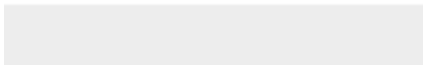
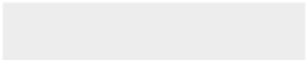


Click here to access/download  
**Supplemental Coding Files**  
LightCurve.csv





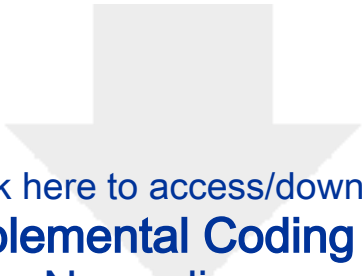
Click here to access/download  
**Supplemental Coding Files**  
HEALPixRandom.py



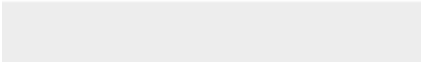



Click here to access/download  
**Supplemental Coding Files**  
LinearRegression.py

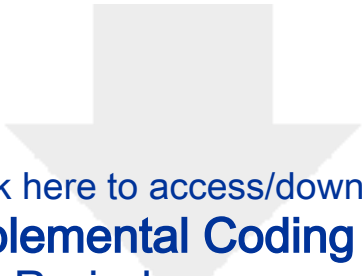




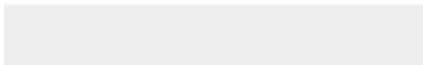

Click here to access/download  
**Supplemental Coding Files**  
Normalize.py








Click here to access/download  
**Supplemental Coding Files**  
Periodogram.py



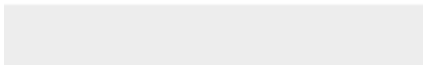



Click here to access/download  
**Supplemental Coding Files**  
PlotCovariance.py





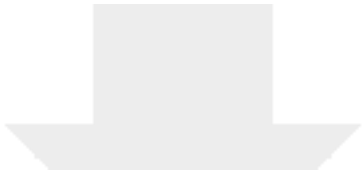
Click here to access/download  
**Supplemental Coding Files**  
PlotMap.py



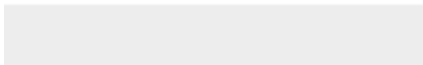
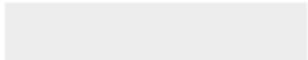


Click here to access/download  
**Supplemental Coding Files**  
PlotPeriodogram.py





Click here to access/download  
**Supplemental Coding Files**  
PlotSVD.py



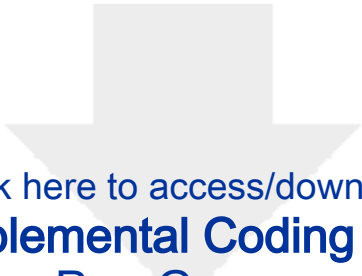


Click here to access/download  
**Supplemental Coding Files**  
PlotTimeSeries.py

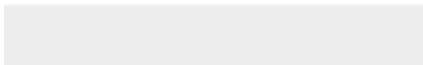
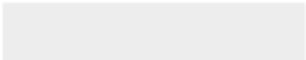


Click here to access/download  
**Supplemental Coding Files**  
PlotWeight.py





Click here to access/download  
**Supplemental Coding Files**  
PrepGeo.py







Click here to access/download  
**Supplemental Coding Files**  
SingularValueDecomposition.py





Click here to access/download  
**Supplemental Coding Files**  
ComputeWeight.py





Click here to access/download  
**Supplemental Coding Files**  
Covariance.py